frontiers in Materials

REVIEW
published: 01 July 2021
doi: 10.3389/fmats.2021.668834

The Application of 3D-Printing and Nanotechnology for the Targeted Treatment of Osteosarcoma

Ayesha Suleman[1], *Pierre P. D. Kondiah*[1], *Mostafa Mabrouk*[2] *and Yahya E. Choonara*[1]*

[1]*Wits Advanced Drug Delivery Platform Research Unit, Department of Pharmacy and Pharmacology, School of Therapeutic Science, Faculty of Health Sciences, University of the Witwatersrand, Johannesburg, South Africa,* [2]*Refractories, Ceramics and Building Materials Department, National Research Centre, Giza, Egypt*

Osteosarcoma is a malignant bone neoplasm prevalent in adolescents. Current therapies include chemotherapy and surgery. Surgical resection of osteosarcoma induces a large bone defect which may be overcome by employing scaffolds for bone tissue engineering. This review details the polymers and bioceramics that may be used to fabricate 3D printed scaffolds for bone regeneration and the nanotechnology strategies that may be incorporated into such scaffolds. Natural polymers discussed include chitosan, alginate, collagen, gelatin, and silk fibroin. Synthetic polymers discussed include polycaprolactone, polyurethane, poly(lactic)acid and poly(vinyl) alcohol. Bioceramics that are utilized in bone regeneration such as calcium phosphate, calcium silicate and bioglass are elaborated on. Furthermore, comparison data between different types of 3D printed scaffolds for bone regeneration are presented. A discussion on Photo-responsive and magneto-responsive 3D printed scaffolds that have been fabricated for bone regeneration is included. Research concerning drug-loaded scaffolds as well as the incorporation of nanocarriers into scaffolds for bone regeneration is provided. Chemotherapy utilized in osteosarcoma therapy has severe adverse effects due to being non-selective between healthy cells and tumor cells. A possible way to overcome this is to utilize nanotechnology. Therefore, research detailing other types of nanocarriers that have the potential to be incorporated into 3D printed scaffolds for localized adjuvant therapy is presented.

Keywords: 3D printing, osteosarcoma, nanotechnology, bone regeneration, polymeric platforms

OPEN ACCESS

Edited by:
Jinguang Hu,
University of Calgary, Canada

Reviewed by:
Antonio Greco,
University of Salento, Italy
Hitendra Kumar,
University of British Columbia Okanagan, Canada

***Correspondence:**
Yahya E. Choonara
Yahya.Choonara@wits.ac.za

Specialty section:
This article was submitted to Polymeric and Composite Materials, a section of the journal Frontiers in Materials

Received: *17 February 2021*
Accepted: *22 June 2021*
Published: *01 July 2021*

Citation:
Suleman A, Kondiah PPD, Mabrouk M and Choonara YE (2021) The Application of 3D-Printing and Nanotechnology for the Targeted Treatment of Osteosarcoma. Front. Mater. 8:668834. doi: 10.3389/fmats.2021.668834

INTRODUCTION

Osteosarcoma is a malignant neoplasm of which there is osteoid formation by tumor cells (Heck and Toy, 2017). According to the American Cancer Society, osteosarcoma is prevalent in patients between the ages of 10 and 30. Those diagnosed with osteosarcoma over the age of 60, consist of 10% of the population afflicted (The American Cancer Society, 2020). Osteosarcoma may arise from certain predisposing factors such as Paget's disease, exposure to radiation, chemotherapy, genetics as well as foreign bodies inserted into bone such as orthopedic implants. The majority of osteosarcomas occur in long bones, close to the joint areas (proximal areas of the humerus and tibia, and the distal areas of the femur). Osteosarcomas are less prevalent in flat bones and the spine (Reith, 2018).

Current therapy for osteosarcoma employs the administration of neoadjuvant chemotherapy followed by surgery and adjuvant chemotherapy. Adjuvant chemotherapy is utilized after surgical removal of

osteosarcoma to mitigate the risk of tumor micro metastases. The most common chemotherapeutic regimen for osteosarcoma consists of methotrexate, doxorubicin and cisplatin (Chou et al., 2008; Luetke et al., 2014). These chemotherapeutic agents vary in severe adverse effects, including irreversible ototoxic and nephrotoxic complications (cisplatin), myelosuppression and mucositis (methotrexate), cardiotoxicity and tissue necrosis (doxorubicin) (Toy and Heck, 2017). These adverse effects are prevalent as chemotherapeutics do not differentiate between healthy, normal cells and tumor cells. Surgery is a critical component in the treatment of osteosarcoma. The current approach to replace bone after surgery is to employ bone grafts. Bone grafts may be autogenous (from the patient's own body), homogenous (from other humans), xenografts (from other species). Each of these approaches has its own limitations, therefore research has been focused on the use of safer, more cost-effective synthetic grafts (Martin and Bettencourt, 2018).

Synthetic osteo-regenerative scaffolds should be biocompatible and have the appropriate porosity, degradability, compositional and mechanical properties to be suitable for bone regeneration as bone regeneration is a complex process as molecular, biochemical, mechanical and cellular aspects have to be considered (Wang C. et al., 2020).

3D printing is an advantageous method to fabricate implantable scaffolds for bone regeneration. 3D printed scaffolds can be precisely designed to mimic bone tissue morphologically (Wang C. et al., 2020) and provides control over scaffold pore shape, size (Ghorbani et al., 2020), and facilitates the incorporation of other functional agents within the scaffold (Wang C. et al., 2020).

In addition, one of the strategies to target the delivery of chemotherapeutic compounds in osteosarcoma has been to employ nanocarriers. For example, targeted nanoparticles can increase the bioavailability and stability of chemotherapeutics while reducing the risks of side effects (Raj et al., 2019). Selective and precise release of chemotherapeutic compounds may also be achieved by the employment of stimuli-responsive nanoparticles. In addition, nanocarriers can be designed to release chemotherapeutic drugs according to triggers such as intrinsic stimuli (Wang S.-Y. et al., 2020).

This review details the 3D printing and nano-enabling of synthetic and natural polymers as well as bioceramics that have been researched as potential candidates for targeted bone regeneration in Osteosarcoma. In particular, magneto- and photo-responsive scaffolds for application in osteosarcoma are discussed as well as a concise incursion into nanoparticles that have been incorporated into scaffolds for targeted bone regeneration. Nanoparticles that have the potential to be incorporated into osteo-mimetic scaffolds for localized adjuvant therapy are also elaborated on.

FABRICATION OF 3D-PRINTED SCAFFOLDS FOR ENHANCED BONE REGENERATION

Among the techniques used to fabricate 3D printed scaffolds, extrusion printing is most popular for bone regeneration (Martínez-Vázquez et al., 2015; Bendtsen et al., 2017; Fahimipour et al., 2017; Pei et al., 2017; Kim H. et al., 2018; Luo et al., 2018; Du et al., 2019; Martin et al., 2019). Other techniques that have been employed include Fused Deposition Modeling (FDM) (Rajzer et al., 2018; Chen et al., 2019; Liu et al., 2020), Binder Jet Printing (Sarkar and Bose, 2019), Melt Electrohydrodynamic 3D Printing (Bai et al., 2020) and Selective Laser Sintering (Feng et al., 2020; Shuai et al., 2020).

Bone is a dynamic and complex tissue consisting of a hard matrix. Two components contribute to the matrix of bone—mineral (majority in the form of hydroxyapatite) and matrix proteins (the main protein being collagen type I). Bone consists of two types of cells—the osteoblast family and osteoclasts. The osteoblast family includes osteoblasts (which form bone by depositing mineral). Once surrounded by bony matrix the osteoblasts are referred to as osteocytes (which maintain bone). Osteoclasts resorb (remove) bone tissue. Together, these cells continuously remodel and maintain bone (White et al., 2012). Structurally, human bone tissue consists of cancellous and cortical bone. Cancellous bone is spongy-like with a high porosity at 50–90% and accounts for 20% of the human skeleton. Cortical bone makes up 80% of the weight of the human skeleton with a porosity of 5–10%. Cortical bone has a greater Young's modulus and compressive strength than cancellous bone (Zhang et al., 2014). Cortical bone possesses the ultimate strength of 30–211 MPa and an elastic modulus of 16–20 GPa. Cancellous bone on the other hand has the ultimate strength of 51–193 MPa and an elastic modulus of 4.6–15 GPa (Huang et al., 2014). **Figure 1** illustrates the hierarchical structure of bone tissue.

In general, there are five therapeutic targets that bone regeneration scaffolds aim for; 1) growth factors (osteoinduction), 2) vascularization (angiogenesis), 3) mechanical properties, 4) osteogenesis and 5) osteoconduction. These five targets form part of the "diamond concept" developed by Giannoudis et al. (2007, 2008). Scaffolds for bone regeneration should possess at least three of these five properties. (Giannoudis et al., 2007; Giannoudis et al., 2008; Jahan and Tabrizian, 2016). When a scaffold is referred to as "osteoconductive" it facilitates the ingrowth of mesenchymal stem cells (MSCs), perivascular tissue and capillaries. When a scaffold is referred to as "osteoinductive", it facilitates the recruitment and differentiation of MSCs into osteoblasts and chondroblasts which leads to new bone formation. Osteoinduction is modulated by growth factors such as bone morphogenetic proteins (BMP) -2, -4 and -7 and vascular endothelial growth factor (VEGF). Osteogenesis is the synthesis of new bone by viable cells (Khan et al., 2005; Roberts and Rosenbaum, 2012).

Several researchers have studied and reviewed the effects of porosity and pore size on angiogenesis, cell behavior during ossification, mechanical and degradation properties and concluded that scaffold pore size and porosity may influence ossification, angiogenesis as well as mechanical and degradation properties. Scaffolds that are microporous (100–600 μm) displayed superior vascularization and integration with the bone tissue of the host. Increased pore size increased bone ingrowth (and therefore osteoconduction). Angiogenesis was supported by triangular, rectangular and elliptic pores while

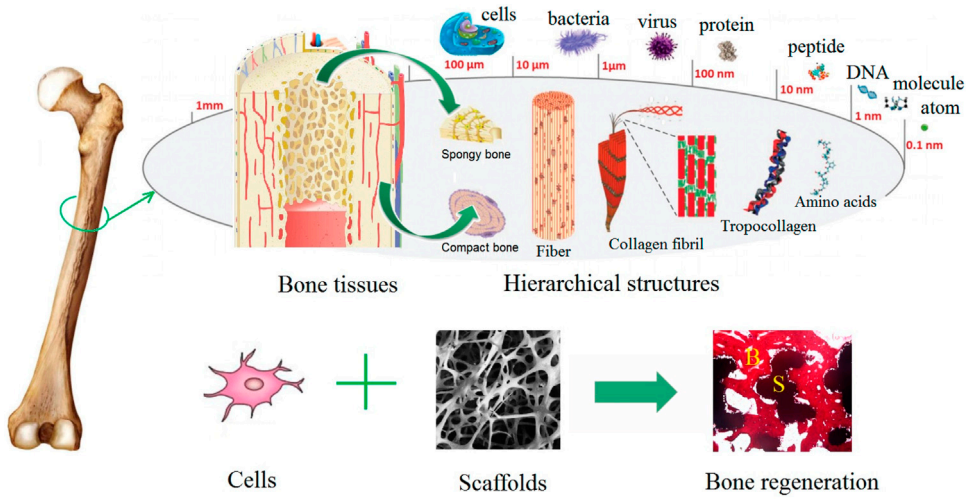

FIGURE 1 | Illustration of the hierarchical structure of bone. Reproduced from Chen X. et al. (2018) under Creative Commons Attribution (CC BY) license (CC BY 4.0) (https://creativecommons.org/licenses/by/4.0/).

TABLE 1 | Combinations of polymers and bioceramic composite scaffolds and their properties.

Polymer/s	Bioceramic	Drug	Properties	References
Chitosan/PVA	Hydroxyapatite	BMP-2	BMP enhanced proliferation and attachment of cells Mechanical strength- elastic modulus of 91.14 MPa	Ergul et al. (2019)
Alginate/gelatin	Hydroxyapatite	—	Nanoapatite increased proliferation and osteogenic differentiation Nanohydroxyapatite increased mechanical strength of scaffolds	Luo et al. (2018)
Alginate	—	BFP-1	*In vitro*: Cell viability, migration, proliferation *In vivo*: accelerated bone regeneration	Heo et al. (2017)
Collagen/decellularized extracellular matrix (dECM)/Silk Fibroin (SF)	—	—	Collagen/dECM and Collagen/dECM/SF scaffolds displayed better cell proliferation and differentiation compared to pure collagen scaffold Collagen/dECM/SF had better mechanical strength	Lee et al. (2018)
Gelatin/PVA	—	—	Cell proliferation and differentiation Mechanical strength	Kim H. et al. (2018)
Silk Fibroin/sodium alginate	Hydroxyapatite	Bovine serum Albumin	Cell attachment and migration Increased SF/HA ed to increased cell proliferation	Huang et al (2019)
PCL	β-tricalcium phosphate	—	β-tricalcium phosphate enhanced proliferation and differentiation Mechanical strength	Bruyas et al. (2018)
Piperazine based- polyurethane-urea	—	—	Osteoconductive Sufficient mechanical strength	Ma et al. (2019)
PLLA/MgO/Halloysite nanotubes	—	—	Cell adhesion, proliferation, migration facilitated Mechanical strength	Liu et al. (2020)
PVA	Biphasic Calcium Phosphate	Platelet rich fibrin (PRF)	*In vitro*: scaffolds with PRF promoted greater cell adhesion, proliferation and differentiation *In vivo*: scaffolds with PRF stimulated greater bone formation	Song et al. (2018)

mechanical strength was improved by square pores. Smaller pores, staggered orientation of pores and a gradient porosity provided greater mechanical strength (compressive modulus). Larger pore size was associated with faster degradation rates (Abbasi et al., 2020). Zaharin and co-workers 3D printed titanium alloy scaffolds (Ti6Al4V) with cube and gyroid pore structures. The scaffold's pore sizes ranged between 300 and 600 μm. Interestingly, in this study, pore size was the deciding factor of whether the scaffold displayed similar properties to bone. It was concluded that scaffolds of both pore geometries showed similarity to natural bone properties at a pore size of 300 μm (Zaharin et al., 2018). Pore structure and size impact the mechanical strength of scaffolds. Zhao and coworkers researched the effect of honeycomb structured pores on the mechanical strength of 3-D printed polylactic acid and photosensitive resin scaffolds. PLA scaffolds with honeycomb structure displayed a greater compressive modulus. It was also suggested that a smaller pore size be used when designing scaffolds to improve mechanical strength (Zhao et al., 2018). Hence, the geometry and physical characteristics of scaffolds such

as curvature, pore size and shape need to be carefully controlled to enhance mechanical strength and cellular responses for effective bone tissue regeneration.

Most polymers and bioceramics are therefore used in combination to form composite scaffolds due to individual polymers lacking the required properties for optimal bone tissue regeneration. **Table 1** provides a list of selected combinations of polymer-ceramic composite scaffolds that have been explored.

Natural Polymers Used for 3D-Printing of Scaffolds in Bone Regeneration

3D-Printed Chitosan Scaffolds

Chitosan is a natural biopolymer (Ahmed et al., 2015; Saravanan et al., 2016) that can be 3D-printed with appropriate binders. Chavanne et al. (2013) explored various binders such as citric acid, lactic acid and acetic acid on chitosan/hydroxyapatite composites. Due to high wettability, medium viscosity and short solidification time lactic acid (40% wt.) was found to be an optimal binder (Chavanne et al., 2013).

Native chitosan poses some limitations for fabricating scaffolds in bone regeneration due to its limited potential to repair bone defects. These limitations include poor antimicrobial activity, quick depolymerization that occurs *in vivo,* poor water solubility and hemo-incompatibility. Therefore, chemical modifications such as phosphorylation, carboxyalkylation, hydroxylation, quaternization, copolymerization and sulfation may be necessary (Logithkumar et al., 2016) and should be considered when 3D printing chitosan scaffolds for application in bone tissue engineering. Combining chitosan with other polymers (such as alginate and gelatin), ceramics (such as hydroxyapatite) and other materials (such as silicon dioxide) can assist with attaining the desired chemical and biological properties required for bone tissue regeneration (Saravanan et al., 2016).

Caballero et al. (2019) studied the relationship between rheology and the composition of chitosan/calcium phosphate inks. It was shown that the higher the concentration of chitosan, the greater the 3D-printability of the ink. The polymer chain entanglement was influenced by chitosan. With higher chitosan concentrations, the ink had more structure (i.e., more viscous), less Newtonian in nature and displayed increased shear thinning behavior. The calcium phosphate morphed from dicalcium phosphate dihydrate into hydroxyapatite that was mineralized in the chitosan scaffold upon printing in basic water/ethanol baths. In addition to the chitosan concentration, the properties of the inks depended on the inorganic to organic ratio. The inorganic to organic ratio influenced the ionic strength and mineral content of the inks. While chain entanglement and mineral content resulted in the ink being less Newtonian, increasing the ionic strength made the ink more Newtonian. The chitosan/calcium phosphate inks were used to fabricate 3D printed scaffolds by robocasting (Caballero et al., 2019).

In another study, chitosan and chitosan/hydroxyapatite hydrogels laden with MC3T3-E1 pre-osteoblast cells were compared with alginate and alginate/hydroxyapatite hydrogels. In terms of cell differentiation and proliferation, chitosan was regarded to be superior compared with alginate. These hydrogels were printed by an extrusion based printer (Demirtaş et al., 2017).

3D-Printed Alginate Scaffolds

Alginate is a biopolymer derived from brown algae (Venkatesan et al., 2015) and may require further purification for application in bone regeneration applications (Torres et al., 2019). Alginates form hydrogels by ionic crosslinking with divalent cations and can be used as bioinks to form 3D-printed scaffolds (Hernández-González et al., 2020). Typically, alginate is deficient in biological properties that can precipitate bone formation (Park et al., 2018), neither does it have sufficient mechanical strength (Venkatesan et al., 2015). However, alginates have been still used in bone regeneration as they are suitable vehicles for the delivery of peptides such as BFP-1 (Heo et al., 2017). Introducing sulfate groups to alginate in bio-inks for 3D printing has shown to prolong BMP-2 activity (Park et al., 2018). To overcome the lack of mechanical properties, alginate may be used in combination with other natural or synthetic osteo-compatible biopolymers used in bone regeneration (Venkatesan et al., 2015).

Bendtsen et al. (2017) studied various concentrations of 3D printable hydrogels comprising alginate, polyvinyl alcohol (PVA) and hydroxyapatite. Two hydrogels had optimized printing quality. Among the two optimized hydrogels, the hydrogel constituting 2.5% alginate, 0.15% Na_2HPO_4, 0.20% $CaSO_4$, 2.5% hydroxyapatite and 0.72% NaCl possessed the optimal 3D-printing quality when developed with cell culture media. The presence of PVA and hydroxyapatite within the alginate hydrogel contributed significantly towards the printability, viscosity and cell viability. These hydrogels were fabricated by extrusion printing. (Bendtsen et al., 2017). In addition, Luo et al. (2017) fabricated 13-93 bioactive glass/alginate scaffolds composed of different mass ratios by extrusion printing. The mass ratios of 13-93 bioactive glass: alginate were 4:4, 2:4, 1:4 and 0:4. When compared to the pure alginate scaffold, the scaffolds that contained 13-93 bioactive glass had increased apatite mineralization and improved mechanical strength. The presence of bioactive glass within the scaffold also improved scaffold porosity and pore size. Optimal mechanical strength, and the highest proliferation and attachment of rat bone mesenchymal stem cells (rBMSCs) was found in the scaffold consisting of mass ratio 2:4 (Luo et al., 2017). These are classical examples of combining alginate with biomaterials having superior mechanical strength to render alginate suitable for the fabrication of 3D-printed bone regenerative scaffolds. However, based on the values provided above for cortical and cancellous bone regeneration, further improvements have to be made to enhance the mechanical strength of alginate scaffolds to facilitate implantation at load-bearing sites.

3D Printed Collagen Scaffolds

Collagen (type I) is secreted by osteoblasts and is the most abundant type of collagen found in the extracellular matrix (ECM) of bone (Boskey, 2003; Ferreira et al., 2012). Collagen is osteoconductive, has weak antigenicity (Ferreira et al., 2012; Zhang et al., 2018) and is the most abundant organic component

of bone; therefore it serves as an excellent mineralization template. Collagen also provides a surface for cell adhesion (Zhang et al., 2018). However, native collagen is deficient in mechanical strength And therefore may be combined with other biopolymers to increase the mechanical strength and achieve enhanced cellular activity (Lee et al., 2018). In a study by Montalbano et al. (2018), 3D-printed scaffolds fabricated from collagen Type I (with bioactive components such as mesoporous bioactive glass containing strontium) were combined to form a hybrid system. Interestingly, the results of the bioactivity studies displayed that the bioactivity of the constructs may be enhanced due to the acidic groups of the collagen fibers providing increased sites for hydroxyapatite nucleation (Montalbano et al., 2018).

Lin et al. (2016) fabricated chemical and solvent-free collagen/hydroxyapatite scaffolds by robocasting. The hydroxyapatite powder used measured <100 nm in particle size. Optimal printing parameters were established as rods of 600 μm in diameter for moderate mechanical strength and bone regeneration outcomes. Non-printed scaffolds were compared to 3D printed scaffolds. Non-Printed scaffolds were prepared by filling molds with ink utilized for the 3D printed scaffolds. The molds matched the dimensions and shape of the 3D printed scaffolds. The ink filled molds were then lyophilized to form non-printed scaffolds. The results displayed that when compared *in vitro*, 3D printed scaffolds improved cell proliferation and differentiation. When compared *in vivo* the 3D printed scaffolds facilitated cell migration, osteogenesis and enhanced repair. However, despite possessing moderate mechanical strength, the scaffolds were still deemed as suitable for application only in bone defects with low load-bearing capacity or cancellous bone (Lin et al., 2016). This may not be suitable for application in post-surgical resection of osteosarcoma of the tibia or femur due to the load-bearing nature of the bone.

A collagen-based scaffold by use of indirect 3D printing was developed by Sachlos et al. (2006). Nano-sized carbonate substituted hydroxyapatite crystals with dimensions of approximately 180 × 80 × 20 nm were precipitated within collagen fibers. This was achieved by enlisting a biomimetic precipitation technique. A calcium chloride solution served as the source of calcium while potassium dihydrogen phosphate served as the phosphate source. These two solutions were separated by a collagen membrane and precipitated within the membrane as carbonate substituted hydroxyapatite crystals. The collagen membranes were air-dried after precipitation was allowed to occur, then shredded into flakes and mixed in a collagen dispersion. This mixture was then cast into 3D printed molds that were fabricated by hot-melt inkjet printing. The mold could facilitate the formation of microchannels that would permit the perfusion of the scaffold. However, appropriate mechanical testing, *in vitro* cell studies and *in vivo* experiments were not conducted (Sachlos et al., 2006). Appropriate testing will have to be conducted to prove that this scaffold meets at least three of the five criteria mentioned in the diamond concept and will have to prove sufficient mechanical strength if scaffolds of this nature is to be considered for application of post-surgical resection of osteosarcoma.

3D Printed Gelatin Scaffolds

Gelatin is a derivative of collagen synthesized by partial acid (type A) or alkaline (type B) hydrolysis from animal collagen. (Djagny et al., 2001; Hoque et al., 2015). Type A gelatin can be employed as a vehicle for acidic proteins *in vivo*, while type B has been used for the prolonged release of basic molecules (Echave et al., 2017). To improve the thermal and mechanical properties of gelatin for *in vivo* applications, crosslinking of gelatin is necessary (Yang et al., 2016). Compared to collagen, gelatin displays lower immunogenicity (Santoro et al., 2014; Echave et al., 2017) and has several positive traits such as elasticity and cell-adherence due to the RGD sequences present in its primary structure (Su and Wang, 2015). When gelatin is extracted at a reduced temperature, greater mechanical strength is obtained but not sufficient for application in bone tissue engineering or regeneration (Usta et al., 2003; Kuttappan et al., 2016).

To overcome this, Kim H. et al., (2018) fabricated combined gelatin/PVA scaffolds by extrusion printing using different gelatin: PVA ratios. The pure gelatin scaffold displayed exceptional protein and water absorption capabilities and the optimal gelatin: PVA ratio for cell differentiation, cell proliferation and mechanical strength was established to be 5:5 (Kim H. et al., 2018). Hydroxyapatite/gelatin scaffolds were also fabricated by extrusion printing by Martinez-Vazquez et al. (2015). In their study, hydroxyapatite was doped with silicone and the average size of the hydroxyapatite-silicone crystals was 35 ± 5 nm. The presence of gelatin within the scaffold resulted in an increase in cell differentiation when compared to pure ceramic scaffolds. The mechanical characteristics of the scaffolds were similar to trabecular bone tissue (Martínez-Vázquez et al., 2015) and thus may not be suitable for application in post-surgical resection of osteosarcoma in load-bearing bones.

In another study by Celikkin et al. (2019), 3D-printed gelatin methacrylate hydrogel scaffolds containing gold nanoparticles (AuNP) were fabricated by extrusion printing. AuNPs were included to enhance Computed Tomography (CT) imaging. The study also researched the impact of different AuNP sizes and concentrations on scaffold cytocompatibility and mechanical properties. The optimal hydrogel formulation was determined to contain AuNPs of 60 nm in size and 0.16 mM concentration. This formulation was then utilized to fabricate 3D printed scaffolds to assess the behavior of Mesenchymal stem cells. Cell studies indicated that both gelatin methacrylate scaffolds with and without AuNPs successfully facilitated osteogenic differentiation. The scaffolds containing AuNPs also enhanced μCT imaging (Celikkin et al., 2019). The inclusion of AuNPs to enhance CT imaging may be of advantage in monitoring the bone regeneration and healing process after scaffold implantation into the resected tumor site.

3D Printed Silk Fibroin Scaffolds

Silk is a proteinaceous biopolymer (Melke et al., 2016; Bhattacharjee et al., 2017; Ma H. et al., 2018) commercially available from two families of silk worms. Silk fibroin from the tropical tasar silkworm possesses the RGD peptide sequence that facilitates superior cell adhesion (Datta et al., 2001; Bhattacharjee et al., 2017). In bone regeneration silk

protein is advantageous in that it possesses mechanical strength and biodegradability. Silk fibroin systems have slow degradation while maintaining their load-bearing capacity (Ma H. et al., 2018). Mulberry silk in particular has a Young's Modulus of 12.4–17.9 GPa (Pérez-Rigueiro et al., 2001; Melke et al., 2016). However, these mechanical characteristics cannot be compared to silk fibroin processed into scaffolds as their mechanical characteristics will differ depending on the process parameters used to form the scaffold (e.g., matrix stiffness, processing techniques and composition) (Melke et al., 2016).

A study by Huang et al. (2019) researched combined 3D printed silk fibroin/hydroxyapatite scaffolds. Silk fibroin/hydroxyapatite nanocomposites of <100 nm in width were prepared by co-precipitation. The nanocomposites were combined with sodium alginate to form a bio-ink and were 3D printed by extrusion. The mechanical strength of the 3D printed silk fibroin/hydroxyapatite scaffolds demonstrated that they were suitable for trabecular bone applications. However, when compared to hydroxyapatite/sodium alginate scaffolds, scaffolds containing increased amounts of silk fibroin/hydroxyapatite nanocomposites displayed poorer mechanical strength. The scaffolds with higher silk fibroin/hydroxyapatite facilitated greater cell proliferation and osteogenic differentiation. (Huang et al., 2019).

In a study employing pure collagen, collagen/decellularized ECM and collagen/dCEM/silk fibroin scaffolds, the 3D printed scaffolds with silk fibroin displayed the most potential for bone regeneration due to superior mechanical properties, increased cell viability and increased preosteoblast cell deposition of calcium (Lee et al., 2018). However, the mechanical strength of these scaffolds may not be suitable for application in post-surgical resection of osteosarcoma at load-bearing sites.

Synthetic Polymers Used for 3D-Printing of Scaffolds in Bone Regeneration

3D Printed Polycaprolactone Scaffolds

Polycaprolactone (PCL) is a semi-crystalline polymer that is suitable in bone tissue engineering due to its prolonged biodegradation rate (2–3 years) (Dwivedi et al., 2020). Although not osteoconductive, PCL may be modified to obtain osteoconductivity and osteoinductivity, for example, by incorporation of growth factors (Mantila Roosa et al., 2010). 3D printed PCL scaffolds are available as bioresorbable implants used in craniofacial surgery (Prasadh and Wong 2018). The mechanical properties and osteoinductivity of PCL can be improved by the addition of β-tricalcium phosphate. Bruyas et al. (2018) observed that the concentration of β-tricalcium phosphate influenced the mechanical properties of the scaffolds fabricated by FDM. PCL scaffolds containing 0, 20, 40, and 60 wt% β-tricalcium phosphate displayed a Young's Modulus of 264, 355, 495, and 1,140 MPa, respectively. Furthermore, by adjusting the β-tricalcium phosphate concentration, the biodegradation ratio can be optimized (Bruyas et al., 2018). The mechanical strength and osteoconductivity of these scaffolds make it a potential candidate for application in post-surgical resection of osteosarcoma, however, at least one other criteria of the diamond concept has to first be observed.

Heo et al. (2019) developed 3D printed PCL scaffolds coated in fish bone extract. The scaffolds were first fabricated by extrusion of melted PCL pellets then soaked in 1 and 3 wt% fish bone extract solutions. Native PCL scaffolds, as well as scaffolds coated with fish bone extract, exhibited similar mechanical properties suitable for bone regeneration. Scaffolds coated in fishbone extract had increased cell proliferation, calcium and phosphorous deposition and osteoblast differentiation (Heo et al., 2019).

Kim J.-Y. et al. (2018) researched the fabrication of 3D printed PCL scaffolds incorporated with β-tricalcium phosphate and bone-derived decellularized ECM (bone dECM) derived from porcine. The PCL and PCL-β-tricalcium phosphate scaffolds were first fabricated by extrusion printing at 120 °C and then immersed in bone dECM solution followed by incubation and lyophilization. *In vitro* studies conducted with the 3D printed scaffolds coated in bone dECM demonstrated excellent cell seeding, proliferation and differentiation. *In vivo* studies demonstrated that scaffolds decorated with bone dECM displayed bone tissue growth within the scaffold. 3D printed scaffolds without bone dECM only had bone tissue growth on the edges of the scaffolds whereas those with bone dECM displayed greater mineralization and osteoid formation. The scaffolds also mimicked the mechanical properties of human cancellous bone (Kim J.-Y. et al., 2018).

In another study, 3D printed PCL scaffolds were fabricated by FDM into different geometries namely, honeycomb, gyroid and mesh structures. These 3D printed scaffolds were then loaded with hydrogels formulated from alginate and gelatin and the hydrogel retention capabilities of the different scaffold structures were researched. The gyroid structured 3D printed PCL scaffold retained the most hydrogel and was selected for further research. Apatite formation increased within the hydrogel, whereas smaller apatite formation was noted on PCL surfaces, which reduced over time due to dissolution. The PCL-gel scaffold displayed cytocompatibility, adhesion and viability of cells (Hernandez et al., 2017).

3D Printed Polyurethane Scaffolds

Polyurethanes are biopolymers that comprise hard segments formed by the reaction between a chain extender and a diisocyanate; and the soft segments are formed from olygodiols and diisocyanates (Marzec et al., 2017). The properties of polyurethanes are influenced by its hard-soft segment ratio. One study indicated that as the ratio of hard segments increased, the hydrophilicity of the polyurethane surface increased as well as cell proliferation of human bone-derived cells. However, an increase in hard segments of polyurethane decreased the osteogenic potential (Bil et al., 2009). The properties of polyurethanes can be tailored by manipulation of chemical composition and synthesis technology and parameters. Polyurethanes are non-toxic, promote calcification *in vivo*, possess mechanical and physicochemical flexibility and are biocompatible. Their properties can range from thermoplastic to thermosetting and

can be hydrophilic or hydrophobic. Polyurethanes implanted *in vivo* have supported bone regeneration. Polyurethanes can serve as bone void fillers, shape memory scaffolds and drug carriers (Marzec et al., 2017).

Ma et al. (2019) showed that piperazine can regulate the osteogenesis of osteoblasts in a dose-dependent manner, and may enhance the osteoconductivity of 3D printed piperazine-based polyurethane-urea scaffolds. These scaffolds were 3D printed by extrusion printing. The optimal concentration of piperazine was determined to be ~0.5 mM (Ma et al., 2019).

Wang et al. (2018) fabricated biodegradable shape memory polyurethane 3D printed scaffolds by low temperature fused deposition modeling. The soft segments of the polyurethane were formed by PCL diol and PLLA diol. The hard segments were formed from 2,2-bis(hydroxymethyl)propionic acid and ethylenediamine as chain extenders and isophorone diisocyanate. Superparamagnetic iron oxide nanoparticles were incorporated into the polyurethane ink to facilitate shape fixity and osteoinduction. To impart printability, the bio-inks were combined with either gelatin or polyethylene oxide (PEO). They concluded that the presence of superparamagnetic iron oxide nanoparticles promoted osteogenesis and enhanced shape fixity by promoting crystallinity of the PCL and PLLA. Scaffolds containing gelatin had superior cell viability while scaffolds containing PEO had enhanced shape memory capabilities (Wang et al., 2018).

3D Printed Poly (Lactic Acid) Scaffolds

Poly (lactic acid) (PLA) is a thermoplastic biopolymer with properties affected by its stereochemistry. Poly (L-lactic acid) (PLLA) and poly (D-lactic acid) (PDLA) are both semi-crystalline in nature, however, when combined to form poly (D, L-lactic acid), an amorphous polymer is produced. Both PLLA and PDLA have desirable mechanical strength (Narayanan et al., 2016). Due to its hydrophobicity, PLA has slow biodegradation rates but also decreased cell adhesion. It may stimulate inflammatory reactions due to lactic acid build-up upon biodegradation. These limitations may be mitigated by including buffers in the scaffold matrix to counter lactic acid formation and inclusion of other bioactive material to increase cell adhesion and osteoconductivity (Tajbakhsh and Hajiali, 2017). To improve the mechanical strength of PLA, buffering of the lactic acid biodegradation products to improve the osteogenic activity of PLLA, the incorporation of MgO and halloysite nanotubes have been explored. Halloysite nanotubes increased scaffold strength while MgO promoted cell adhesion, proliferation and differentiation. (Liu et al., 2020).

In another study by Mondal et al. (2020), PLA scaffolds were 3D printed by FDM and modified with hydroxyapatite nanoparticles post-fabrication. The 3D printed scaffolds were immersed in a hydroxyapatite mixture and sonicated followed by drying. The average size of the hydroxyapatite nanoparticles was 36 ± 4 nm. The scaffolds were printed at varying orientations of 0°, 45° and 90°. Scaffolds printed at 90° displayed the highest compressive strength. 3D printed scaffolds modified with hydroxyapatite nanoparticles displayed greater mechanical strength as compared to scaffolds without hydroxyapatite nanoparticles, regardless of printing orientations. In addition, the scaffolds modified with hydroxyapatite nanoparticles displayed greater cell adhesion and proliferation (Mondal et al., 2020).

An interesting combination of scaffold fabrication techniques was used to fabricate gelatin/PLLA hybrid layered scaffolds for application in subchondral bone and nasal cartilage reconstruction. FDM was utilized to 3D print a porous PLLA layer of the scaffold, while electrospinning was utilized to develop a gelatin nanofibrous top layer. A bioactive powder (Osteogenon) was incorporated into the gelatin solutions. The layered scaffolds were formed by electrospinning the gelatin solutions directly onto the 3D printed PLLA scaffolds (Rajzer et al., 2018). These scaffolds may have been designed for application in subchondral bone and nasal cartilage reconstruction, however, the combination of scaffold fabrication techniques may be useful in fabricating scaffolds for application in osteosarcoma. Perhaps due to technology constraints, if only certain biomaterials can be 3D printed, other biomaterials can be added to the 3D printed scaffold by other scaffold fabrication techniques.

In one study, 3D printed PLA scaffolds with different pore sizes of 0.50, 1.00 and 1.25 mm were fabricated. Increased cell proliferation was noticed on scaffolds with pore size of 1.25 mm when compared to scaffolds with pore size of 1 mm. Mechanical testing was conducted on bovine bones and compared to mechanical characteristics of the scaffolds. Although the scaffolds displayed lower modulus values compared to bovine bone, it was concluded that the scaffolds could still have the potential to be utilized for bone repair. The reason provided was that during *in vivo* implantation, cells that infiltrate the scaffold would be able to produce extracellular matrix which would aid in mechanical strength (Velioglu et al., 2019).

3D Printed Polyvinyl Alcohol Scaffolds

Polyvinyl alcohol (PVA) is a water-soluble polymer that imbues scaffolds with strength and flexibility (Kim H. et al., 2018; Song et al., 2018). PVA has also been used in 3D printed scaffolds to enhance the viscosity of hydrogels, increase biocompatibility and osteoconductivity (Bendtsen et al., 2017). In a study by Kim H. et al. (2018), PVA was utilized to impart mechanical properties to the scaffold. Native PVA scaffolds displayed the greatest mechanical strength as compared to the other scaffolds (Kim H. et al., 2018).

Chen et al. (2019) developed 3D printed PVA/β-tricalcium phosphate scaffolds by FDM. PVA/β-tricalcium phosphate composites were first synthesized with β-tricalcium phosphate concentrations ranging from 5 to 20%. These composites were then mixed with co-plasticizers and extruded into filaments. It was noted that an increase in β-tricalcium phosphate concentration led to an increase in mechanical strength and cell proliferation (Chen et al., 2019).

In a study conducted by Feng et al. (2020), polyetheretherketone (PEEK) was combined with PVA to form composite scaffolds by selective laser sintering. Graphene oxide (GO) was added to the combination to enhance interfacial bonding between polar PVA and non-polar PEEK. Different ratios of GO 0, 0.5, 1, 1.5 and 2 wt%

loaded within the PEEK/PVA composites were researched. The scaffolds with 1 wt% of GO possessed optimal mechanical properties and was selected for further study. 3D printed PEEK/PVA scaffolds with 1 wt% GO displayed greater cell proliferation and differentiation *in vitro* compared to PEEK/PVA scaffolds. *In vivo* research demonstrated that PEEK/PVA scaffolds with 1 wt% GO did not just promote new bone formation but could accelerate it (Feng et al., 2020).

The mechanical strength in these scaffolds may not be suitable for application in post-surgical resection of osteosarcoma at load-bearing sites. More research is required to impart sufficient mechanical strength to PVA scaffolds for it to be considered for application in osteosarcoma.

Bioceramics Used for 3D-Printing of Scaffolds in Bone Regeneration

3D Printed Calcium Phosphate Scaffolds

Calcium phosphates are a group of bioceramics that includes hydroxyapatite, biphasic calcium phosphate and tricalcium phosphate. Calcium phosphate ceramics are not osteoinductive in solid and non-porous forms but may be rendered osteoinductive by employing surface modification strategies such as forming macroscopic and microscopic pores, ensuring appropriate scaffold roughness and surface morphology (Samavedi et al., 2013). The osteoinductivity of calcium phosphates is also dependent on surface charge and chemistry of calcium phosphates (Samavedi et al., 2013; Xiao et al., 2020). Phosphate bioceramics are also bioresorbable (Wei et al., 2009; Venkatraman and Swamiappan, 2020).

3D printed β-Tricalcium phosphate (β-TCP) scaffolds lack mechanical strength. To enhance mechanical strength, microwave sintering of these scaffolds has been explored. Microwave sintering increased densification of the 3D printed scaffolds thereby increasing the strength of the 3D printed β-TCP scaffolds (Tarafder et al., 2013).

The weight % of bioceramics present in a scaffold may also need to be optimized. Ergul et al. (2019) researched various ratios of hydroxyapatite (2.5, 5, 10, and 15 wt%) in 3D printed chitosan/PVA scaffolds. Chitosan and PVA mixtures were first blended followed by the addition of hydroxyapatite solution to obtain the hydrogel. The chitosan/PVA scaffold containing 15% weight of hydroxyapatite displayed superior results in printing quality (Ergul et al., 2019).

Coating a scaffold with nanohydroxyapatite may also lead to an increase in scaffold mechanical strength. Luo et al. fabricated alginate/gelatin scaffolds with nanohydroxyapatite. It was determined that the scaffolds coted in nanohydroxyapatite displayed Young's modulus that was twice that of the scaffolds without the coating. In addition, the presence of the nanohydroxyapatite coating contributed to greater cell proliferation, protein adsorption and osteogenic differentiation (Luo et al., 2018). However, despite the increase in Young's modulus of the scaffold, the mechanical strength of the scaffold may not be suitable for application in post-surgical resection of osteosarcoma at load-bearing sites.

3D Printed Calcium Silicates

Calcium silicate bioceramics have superior mechanical properties compared with calcium phosphate bioceramics. Apatite deposition is induced by the silicon-rich layer present on the bioceramic surface. Silicate bioceramics are bioactive- they have excellent interfacial bonding with natural tissue (Wei et al., 2009; Venkatraman and Swamiappan, 2020). Examples of calcium silicates include: α'_L-dicalcium silicate (Ca_2SiO_4), wollastonite ($CaSiO_3$) and larnite (β-Ca_2SiO_4), diopside ($CaMgSi_2O_6$) and hatrurite (Ca_3SiO_5) (Ribas et al., 2019; Venkatraman and Swamiappan, 2020). The biological and physicochemical properties of 3D printed calcium silicate scaffolds may be improved by the addition of compounds such as CeO_2. When compared to ordinary 3D printed mesoporous calcium silicate scaffolds, 3D printed calcium silicate scaffolds incorporated with CeO_2 displayed enhanced osteoinduction markers as well as enhanced vascularization markers (Zhu et al., 2016).

To improve the mechanical strength of calcium silicate scaffolds, calcium sulfate was incorporated into mesoporous calcium silicate scaffolds. Calcium sulfate hemi-hydrate was incorporated into mesoporous calcium silicate powder by being ground followed by passing through a mesh sieve. The powders were then incorporated into a PCL solution for 3D printing by extrusion followed by hydration process. Calcium silicate scaffolds incorporated with calcium sulfate displayed greater mechanical strength. Despite pure mesoporous calcium silicate scaffolds displaying slightly higher cell viability, there were no significant differences between cell adhesion and proliferation between scaffolds with and without calcium sulfate. The composite scaffolds also facilitated the sustained drug release of dexamethasone (Pei et al., 2017).

In another study, 3D printed calcium silicate scaffolds incorporated with strontium were developed. Calcium silicate powder and strontium doped calcium silicate powders were mixed with ethanol and added to melted PCL for 3D printing by extrusion. 3D printed calcium silicate scaffolds containing strontium displayed a 2-fold increase in mechanical strength. *In vitro* studies demonstrated the osteoinductive ability of calcium silicate scaffolds containing strontium. *In vivo* studies demonstrated the capability of the scaffolds containing strontium to promote angiogenesis and osteogenesis (Chiu et al., 2019).

3D Printed Bioactive Glasses in Bone Regeneration

Bioactive glasses may be grouped into silicate-based bioactive glasses, phosphate-based bioactive glasses, borate based bioactive glasses and black glass (Baino, 2018). The most recent generation of bioactive glasses to be developed has been mesoporous bioactive glasses (MBG) by Yan et al. (2004). Bioglasses are osteoconductive and osteoproductive (Rainer et al., 2008).

In a study by Wu et al. (2011), MBG was combined with PVA as a binder for 3D printing. By combining MBG with PVA, the 3D printed scaffolds' toughness was improved and was less brittle. The scaffolds displayed increased mechanical strength as compared to other inorganic scaffolds fabricated by traditional methods and had 200 times the strength of MBG scaffolds

prepared by polyurethane foam templating. The MBG scaffolds also displayed the potential to be utilized for sustained drug release. It was noted that cell proliferation was lower on MGB scaffolds but Alkaline phosphatase activity was higher when compared to control scaffolds (Wu et al., 2011).

In another study, MBG scaffolds were 3D printed by extrusion and also utilized PVA as a binder. However, research was conducted on the removal of PVA post scaffold fabrication to prevent the reduction of MBG's osteogenic potential due to the presence of PVA. The removal of PVA was accomplished by immersion of MBG scaffolds in phosphate-buffered saline solution. This resulted in a biomimetic mineralized layer forming on the surface of the scaffolds as well as throughout the scaffolds. 3D printed scaffolds that underwent immersion displayed an increase in osteogenic related genes and have the potential to accelerate new bone formation (Gómez-Cerezo et al., 2020).

Comparison Between Different Scaffold Compositions

Different bioceramics possess different bone regeneration mechanisms. Therefore, it becomes necessary to develop and compare scaffolds with different bioceramic compositions. Alksne et al. 3D printed PLA/hydroxyapatite and PLA/bioglass composite scaffolds using the FDM technique for comparison of bone regeneration *in vitro*. It was concluded that the PLA/bioglass composite possessed superior osteoinductivity than the PLA/hydroxyapatite scaffolds (Alksne et al., 2020). Feng et al. 3D printed (by extrusion) and compared mesoporous calcium silicate/PCL and mesoporous bioactive glass/PCL scaffolds *in vitro*. The mesoporous bioactive glass/PCL scaffold proved to be superior. By employing 3D printing, an advantage was provided. The comparison of osteogenic properties between the scaffolds were eliminated as highly similar inter-structural and mechanical characteristics were ensured by 3D printing (Feng S. et al., 2019). These studies prompt further research on comparison between scaffolds *in vivo*.

Anbu et al. compared the bone regeneration ability between grafts formed from powdered PLA, 3D printed PLA and commercially available hydroxyapatite–β-tricalcium phosphate. There was bone formation with all three polymers. In the fourth week, the PLA based grafts induced shallow bone formation as compared to the commercially available product. Interestingly, the 3D printed PLA graft was not rejected by healthy living bone-new bone surrounding the graft was observed (Anbu et al., 2019).

These studies prompt more research comparing various composite scaffolds *in vitro* and *in vivo* to determine the superior and optimal 3D printed composite scaffold combinations. Research on scaffolds for application in osteosarcoma should not just focus on osteogenic properties of the scaffolds but rather should strive to incorporate angiogenesis, mechanical strength, osteoconductivity, osteoinductivity and osteogenesis.

Du et al. fabricated and compared 3D printed MBG/SF scaffolds and 3D printed MBG/PCL scaffolds. It was determined that when compared to MBG/PCL scaffolds, the MBG/SF scaffolds had lower degradation ratios, greater mechanical strength, greater *in vitro and in vivo* osteogenic capabilities (Du et al., 2019). **Table 2** summarizes the scaffold composition comparisons and their outcomes.

STIMULI-RESPONSIVE SCAFFOLDS IN BONE REGENERATION

Addressing bone defects induced by surgical resection in osteosarcoma may not be sufficient. There is still a risk of residual tumor cells remaining that may result in the recurrences of osteosarcoma. To address this, Fu et al. 3D printed a bioceramic free carbon-embedding larnite (larnite/C). This was achieved by mixing and 3D printing siliesquioxane silicone and a $CaCO_3$ filler then placing the printed scaffolds under argon atmosphere to undergo ceramic transformation to form larnite/C. The purpose of the free carbon was to facilitate a photothermal effect when stimulated by a NIR laser. The scaffold could successfully destroy human osteosarcoma cells, hindered tumor growth in nude mice and promoted new bone formation *in vivo*. The scaffolds could facilitate the expression of rat bone mesenchymal stem cells *in vitro* (Fu et al., 2020). **Figure 2** depicts the concept of NIR laser used to produce photothermal effects in tumor cells.

Other carbon sources such as graphene oxide may also imbue scaffolds with photothermal conversion properties. Ma et al. developed graphene oxide (GO)-modified β-tricalcium phosphate (GO-TCP) composite scaffolds that displayed photothermal effects even at a low power density of $0.36\ W\ cm^{-2}$. The photothermal effects induces significant MG-63 osteosarcoma cell death *in vitro* and inhibited mice tumor growth. The photothermal temperature of the scaffolds could be modulated by adjusting the concentrations of GO, NIR power densities and surface modification times. Furthermore, the GO-TCP scaffolds displayed better osteogenic differentiation and new bone formation than the plain β-TCP scaffolds (Ma et al., 2016).

Other compounds that have been used in bioceramic scaffolds to imbue scaffolds with photothermal conversion capabilities led to scaffolds with successful photothermal effects and bone regenerating potential. These include, MoS_2 (Wang H. et al., 2020); Fe and Mn (Liu et al., 2018) and $CuFeSe_2$ nanocrystals (Dang et al., 2018). 3D printed Fe-$CaSiO_3$ composite scaffolds were developed and not only displayed anticancer properties due to photothermal ablation but also due to the generation of ROS. The photothermal effect, as well as ROS, had synergistic effects *in vivo* and *in vitro*. The scaffolds also displayed high compressive strength that is suitable for mechanical support in cortical bone defect and displayed bone regeneration potential *in vivo* and *in vitro* (Ma D. et al., 2018).

NIR may have promising results *in vitro* and *in vivo* with small animals such as rats, however, it is uncertain if it can be translated to be effective when applied to humans. Henderson and Morries (2015) endeavored to determine if enough photonic energy from NIR can be delivered to the human brain to precipitate beneficial effects for application in traumatic brain injury and stroke. Their study also included NIR penetration tests using *in vivo* human

TABLE 2 | A summary of the different studies comparing different scaffold compositions and their bone regeneration outcomes.

Scaffold compositions that were compared	Study conducted *in vitro/in vivo*	Outcome	References
PLA/hydroxyapatite vs. PLA/bioglass	*In vitro*	PLA/bioglass scaffolds displayed superior osteoinductive properties	Alksne et al. (2020)
Mesoporous calcium silicate/PCL vs. Mesoporous bioglass/PCL	*In vitro*	Mesoporous bioglass/PCL scaffolds displayed superior osteogenic-related gene expressions	Feng X. et al. (2019)
Commercially available hydroxyapatite–β-tricalcium phosphate vs. powdered PLA vs. 3D printed PLA	*In vivo*	Bone formation was noted with all three groups. However, a significant difference was noted between 3D printed PLA scaffolds and the powdered formulations	Anbu et al. (2019)
Mesoporous bioactive glass/SF vs. Mesoporous bioactive glass/PCL	*In vitro* and *in vivo*	MBG/SF scaffolds had lower degradation ratios, greater mechanical strength, greater *in vitro and in vivo* osteogenic capabilities	Du et al. (2019)

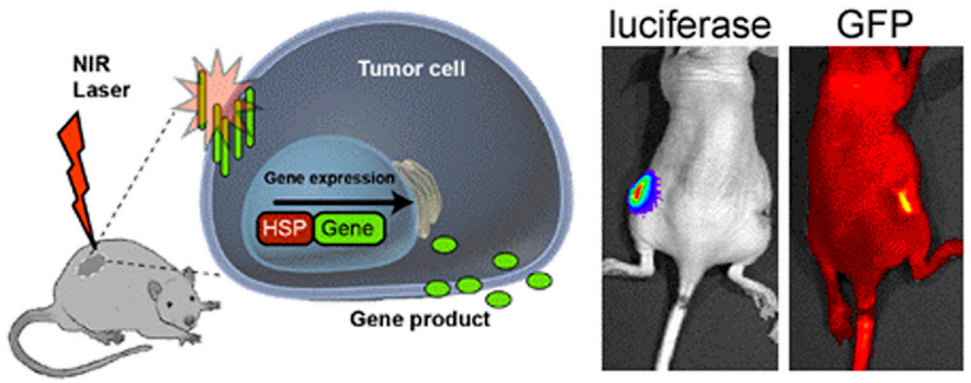

FIGURE 2 | Schematic depicting the use of NIR laser to trigger photothermal effects in tumor cells. HSP- Heat shock protein. Reproduced from Andersson et al. (2014) under Creative Commons Attribution license (CC BY-NC-SA 3.0) (http://creativecommons.org/licenses/by/3.0/).

tissue, through structures such as the hand, ear with cartilage, cheek, subcutaneous flesh and the web of the hand. An 810 nm laser was employed with output setting of 13.5 W for the human tissue *in vivo* study. Several interesting facts were gleaned from their study: i) NIR penetrated better in living tissue due to the lack of post-mortem protein crosslinking; ii) Light may be scattered between the interfaces of different tissue (e.g., fascia and muscle); iii) Pulsed NIR seems to have greater penetration in living tissue as compared to continuous wave NIR. Most importantly, despite the fact that NIR penetration proved to be greater in tissues that contained bone, only over 0.8% of the pulsed NIR energy passed through 2.5–3.0 cm of a living human hand (Henderson and Morries, 2015). Based on this, NIR may not be able to penetrate deep enough with energy for application in osteosarcoma if applied from outside the skin, thus posing a barrier to the use of NIR.

Thus, to facilitate NIR reaching the scaffolds, other routes needed to be explored. Researchers have inserted optical fiber diffusers. A recently published clinical trial employed the use of AuroLase® therapy to treat 16 low-to intermediate risk prostate cancer patients. The treatment occurred over two consecutive days. AuroShells® (Gold-silica nano shells) were administered intravenously on day one and mediated the laser ablation. On the second day, catheters containing optical fiber diffuses were inserted into the tumors, guided by MRI and ultrasound. The optical fiber diffusers facilitated the delivery of NIR to the AuroShells® which resulted in focal photothermal ablation of prostate tumors. After undergoing the procedure, the patients were discharged on the same day. There was minimal damage to the surrounding tissue. Due gastric pain, only one patient did complete the two-day treatment protocol. Of the 15 men that did complete the treatment, 13 men had negative follow-up targeted biopsy results from the targeted ablation zone 12 months after treatment (Rastinehad et al., 2019). In the context of osteosarcoma, the use of optical fibers to facilitate NIR reaching the scaffolds will be accompanied by a major disadvantage in that this would become a very invasive treatment procedure.

Tumor cells may also be destroyed by magneto-thermal therapy. Zhang et al. developed a magnetic scaffold composed of β-TCP–Fe–GO. Nano Fe_3O_4 particles were sandwiched by GO sheets. The sandwich strategy displayed superior magnetothermal efficacy compared to lone Fe_3O_4 nanoparticles on the scaffold surface. The temperature of the scaffolds could be controlled by magnetic intensity and Fe_3O_4 content. GO provided a synergistic effect due its thermal conductivity (Zhang et al., 2016).

The application of a magnetic field to scaffolds may not only be used for magnetothermal purposes. Shuai et al. fabricated

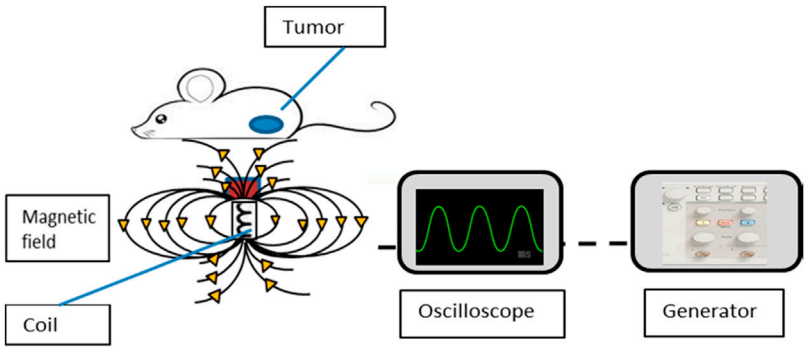

FIGURE 3 | A depiction of how the magnetic field is generated from the coil to affect tumor cells. A generator is connected to a coil and oscilloscope. The generator provides voltage and frequency to the coil while the oscilloscope displays the frequency and amplitude on a screen. Reproduced from Vegerhof et al. (2016) under Creative Commons Attribution (CC-BY) license (CC BY 4.0) (http://creativecommons.org/licenses/by/4.0/).

polyglycolic acid (PGA)/Fe_3O_4 composite scaffolds. Upon applying a self-developed external static magnetic field (SMF), the Fe_3O_4 nanoparticles rearranged according to the SMF resulting in a magnetic field that was locally enhanced. As a result, cell adhesion, differentiation and proliferation were promoted and bone regeneration accelerated (Shuai et al., 2020). **Figure 3** depicts how a magnetic field generated from a coil will interact with a tumor.

3D-Printing of Bioactive-Loaded Scaffolds for Bone Regeneration

To increase the formation of bone, bone regenerative scaffolds may be loaded with bioactives such as drugs, proteins or other compounds. Examples of proteins that have been added to scaffolds include growth factors such as Bone Morphogenic Protein-2 (BMP-2) and Vascular Endothelial Growth Factor (VEGF). Ergul et al. employed BMP-2 to facilitate natural growth of bone cells and to provide easy attachment of cells to the 3D printed chitosan/PVA scaffolds (Ergul et al., 2019). Angiogenesis is crucial in skeletal development and VEGF plays an important role in this regard (Zelzer et al., 2002). VEGF has also been included in a scaffold to enhance angiogenesis, bone repair and growth (Fahimipour et al., 2017). In another study, BMP-2 and VEGF were dual loaded into a 3D printed hydroxyapatite composite scaffold for the combined effects and sustained release of VEGF and BMP-2 (Chen et al., 2020). However, BMP-2 and VEGF have *in vivo* limitations including the potential to elicit immune reactions during prolonged use. Therefore, to overcome these limitations, Yan et al. explored the use of deferoxamine, an iron chelator, loaded into 3D printed PCL based scaffolds. *In vivo* testing displayed that deferoxamine enhances the regeneration of bone and promotes vascular invasion (Yan et al., 2019). The bone regeneration capability of an amino acid peptide derived from BMP-7, called, bone formation peptide-1 (BFP1), was explored in a 3D printed alginate scaffold. BFP-1 enhancement of bone regeneration increases as BFP-1 increases and accelerated bone regeneration was displayed *in vivo* (Heo et al., 2017).

To increase the formation of bone, Zhang et al. incorporated small molecule drugs resveratrol and strontium ranelate into PCL/β-tricalcium phosphate scaffolds. The scaffolds had methacrylated hyaluronic acid and methacrylated gelatin-based hydrogels deposited between the PCL/β-tricalcium phosphate frames. The dual-loaded scaffolds had synergistic effects in enhancing MSC osteogenic differentiation and a combined advantage of promoting angiogenesis and inhibiting osteoclasts. The scaffolds were tested *in vivo* and promoted bone formation. Reservatrol displayed a sustained release profile while Strontium ranelate displayed an initial burst release followed by sustained release. A limitation noted was the erratic release of Strontium Ranelate due to its water solubility (Zhang et al., 2020).

While many studies focus on bone tissue engineering, not many address the need of a scaffold functionalized with antibacterial properties to mitigate the risk of post-surgical infection at the site of scaffold implantation. Therefore, Bai et al. developed a PCL/PEG scaffold, loaded with the antibacterial roxithromycin (Bai et al., 2020). Martínez-Vázquez et al. developed hydroxyapatite/gelatin scaffolds utilising extrusion printing. The hydroxyapatite was doped with silicon. Vancomycin was incorporated within the ink before 3D printing (Martínez-Vázquez et al., 2015). Martin et al. 3D printed a PLA/Collagen/citrate-hydroxyapatite (cHA) scaffold loaded with the antibacterial drug minocycline (Martin et al., 2019). The loading of antibacterial drugs may not be the only approach to fabricating a scaffold with antibacterial properties. The use of silver as an antibacterial compound may also be beneficial (Zhang et al., 2017). However, caution should be exercised that the concentration of silver nanoparticles should not toxic to cells responsible for bone regeneration.

Nano-Enabled 3D-Printed Scaffolds for Bone Regeneration

Zhang et al. proposed a solution to overcome the undesirable release rate of strontium ranelate by encapsulating the compound into microspheres and to load the microspheres in to a bio-ink used for scaffold fabrication (Zhang et al., 2020). To this end,

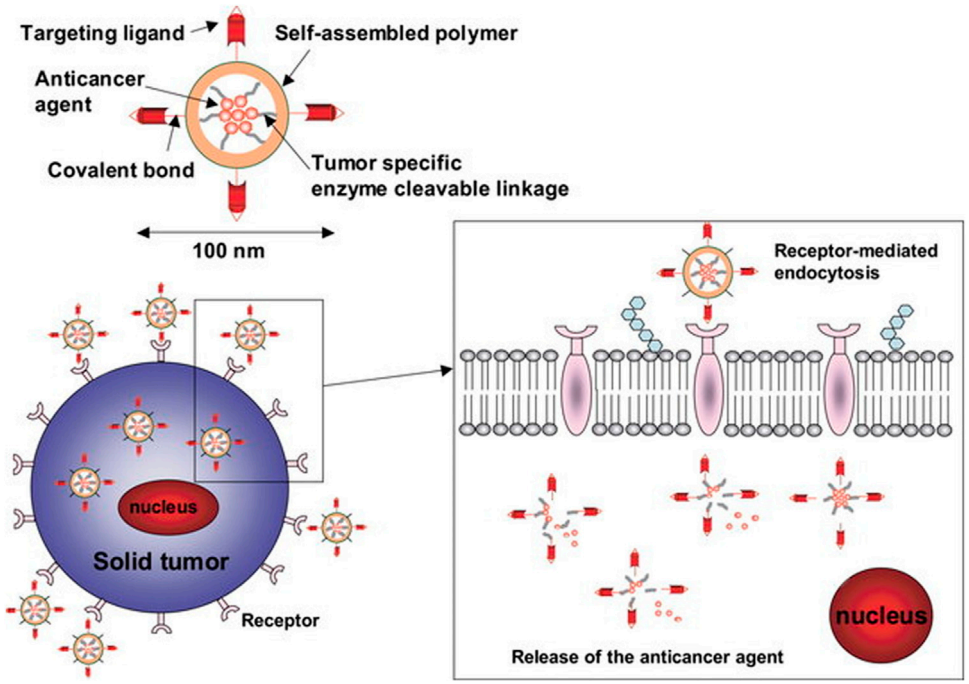

FIGURE 4 | Nanoparticles with ligands for targeted delivery bind to cell receptors to be internalized by receptor mediated endocytosis. Reproduced from Kim and Nie (2005) under Creative Commons Attribution (CC-BY) license (CC BY-NC-ND 3.0) (https://creativecommons.org/licenses/by-nc-nd/3.0/).

nanocarrier-loaded scaffolds were explored as the limitations that many bioactive have such as low solubility and high side effects profile (precipitated by long term use) may be overcome. Furthermore, loading anti-cancer drug-loaded nanoparticles within scaffolds may have application in addressing the problem of residual osteosarcoma cells. **Figure 4** illustrates the different types of nanocarriers that may be incorporated into a 3D printed scaffold. The interaction between the bone and the scaffold is also illustrated.

Nano-Liposomes and 3D-Printed Scaffolds

Liposomes are lipid bilayer spherical nanoparticles with hydrophilic cores (Alavi and Hamidi, 2019). Liposomal carriers are advantageous in many ways. They are highly biocompatible, possess low immunogenicity and prolong the half-life of the drugs they contain (Li Y. et al., 2019). They facilitate the delivery of drugs of various sizes, shapes and solubilities. Hydrophilic drugs can be encapsulated inside the hydrophilic core of liposomes while hydrophobic drugs may be trapped within the lipid bilayer (Alavi and Hamidi, 2019).

Aspirin has displayed positive aspects with regards to bone formation, however, its side effects limit its application for long-term use. Therefore, Li et al. formulated liposomes that had aspirin adsorbed to its surface. These liposomes were loaded into a 3D printed PCL scaffold. Osteoblast differentiation was promoted *in vivo* and *in vitro*. The liposomes were under 200 nm in size and the loading of aspirin had little effect on size and morphology of the liposomes (Li M. et al., 2019). Sarkar and Bose et al. loaded curcumin-encapsulated nanoliposomes into a calcium phosphate 3D printed scaffold. The nanoliposomes were between 40 and 50 nm in size. This bifunctional scaffold not only promoted the formation of healthy bone cells, but also displayed anti-cancer properties (Sarkar and Bose, 2019).

Liposomes that are loaded with anticancer drugs that are standard for adjuvant therapy may also be incorporated into scaffolds for a localized anticancer effect. Below are the anti-osteosarcoma advancements made in liposomes.

Liposomal formulations have been synthesized and studied to address the resistance of osteosarcoma cells to treatment. Caliskan et al. developed dual-loaded Gemcitabine and Clofazimine liposomes. Gemcitabine was encapsulated within the hydrophilic core of the liposomes whereas Clofazamine was trapped within the lipid bilayer of the liposomes. The dual-loaded liposomes displayed a greater cytotoxicity in Saos-2 cells than the individually loaded Gemcitabine and Clofazimine liposomes (Caliskan et al., 2019). In an effort to overcome the resistance of osteosarcoma cells to Doxorubicin, Giansanti et al. demonstrated that vocamine (a plant alkaloid) displays greater efficiency when loaded into cationic liposomes than the free alkaloid in increasing the accumulation of doxorubicin in osteosarcoma cells. The U-2 OS/DX cell line (human multidrug resistant (MDR) osteosarcoma cell line) was employed for this study (Giansanti et al., 2019). Hyaluronic conjugated liposomes containing Hydrogen Sulfide releasing doxorubicin displayed promising results in overcoming doxorubicin-resistant osteosarcoma cells (Gazzano et al., 2019).

There are various FDA approved liposome formulations on the market with indications for various cancers namely; Doxil®,

DaunoXome®, Depocyt®, Myocet®, Mepact®, Marqibo® and Onivyde™. In addition, there are various liposomal formulations available for antifungal therapy, photodynamic therapy and antiviral therapy. Mepact® (approved in 2004) has a specific indication, among other indications, for non-metastatic osteosarcoma (Bulbake et al., 2017).

Polymeric Nanoparticles and 3D Printed Scaffolds

Polymeric nanoparticles are nanoscale, polymer derived drug delivery vehicles. They may be synthesized using one of two methods: i) the "bottom-up" method wherein monomers are polymerized to form the nanoparticles or; ii) the "top down" method whereby polymers are used to synthesize the nanoparticles. Drug loading my occur through absorption, adsorption and entrapment (Choudhury et al., 2019).

Fahimipour et al. developed a gelatin/alginate/β-TCP scaffold 3D printed composite. The scaffold was then loaded with PLGA microcarriers loaded with VEGF. VEGF was encapsulated in PLGA microspheres to facilitate its sustained release (Fahimipour et al., 2017).

Other polymeric nanoparticles loaded with anticancer agents have the potential to be incorporated into scaffolds for bone regeneration. These are the advancements made in polymeric nanoparticles researched for use in osteosarcoma:

Zhao et al. developed polymeric nanoparticles using the top-down method. Paclitaxel was entrapped within the nanoparticles. Pluronic F68 was used as a stabilizer and the nanoparticles were coated with polydopamine. Alendronate was used as a targeting molecule. These nanoparticles were researched on K7M2 wt osteosarcoma cells (Zhao et al., 2019).

To combine the advantages of liposomes and polymeric nanoparticles, lipid-polymer hybrid nanoparticles have also been developed for use in osteosarcoma (Chen F. et al., 2018). To target cancer stem cells and cancer cells in osteosarcoma, nanoparticles tagged with CD 133 aptamers and CL4 were developed to confer CD-133 and Epidermal Growth Factor Receptor targeting. These nanoparticles entrapped the drug salinomycin (Chen X. et al., 2018). To treat osteosarcoma initiating cells, all *trans*-retinoic acid was loaded into hybrid polymer nanoparticles and tagged with CD-133 aptamers to confer CD-133 gene targeting (Gui et al., 2019). Lipid-polymer nanoparticles can be used as a dual-drug loaded vehicle. Lipid-polymer nanoparticles were dually loaded with paclitaxel and etoposide and displayed an efficacy that was two times greater than the free drugs. The dual-loaded lipid-polymer nanoparticles induced greater apoptosis in cells. Decrease cell proliferation was noted in cell groups treated with etoposide and paclitaxel dual-loaded lipid-polymer nanoparticles (Duan et al., 2017).

Iron Oxide Nanoparticles and 3D Printed Scaffolds

Under the section of stimuli-responsive scaffolds, the use of iron to impart magnetic abilities to scaffolds was discussed. However, in addition to magnetic properties iron oxide may exert an anti-cancer effect. Iron oxide nanoparticles induce ROS-mediated toxicity in osteosarcoma cells (Du et al., 2017) and could be used as drug carriers. Popescu et al. conjugated Gemcitabine onto the iron nanoparticles surface. However, the Gemcitabine conjugated iron oxide nanoparticles displayed low cytotoxicity due to decreased cell uptake in MG-63 cells (Popescu et al., 2017). Raghubir et al. loaded riluzole (a glutamate release inhibitor) into iron oxide nanocages and iron oxide nanospheres. The riluzole-loaded nanocages displayed better efficacy as compared to the riluzole-loaded nanospheres in reducing the osteosarcoma tumor size *in vivo* (Raghubir et al., 2020). More research regarding drug loading of Iron oxide nanoparticles with osteosarcoma first line drugs is required.

Due to the potential of iron oxide nanoparticles to agglomerate, strategies need to be developed to modify the surface of the iron oxide nanoparticles. One such strategy, that has been explored, was to coat the iron oxide nanoparticles with Hydroxyapatite (Mondal et al., 2017). Coating iron oxide nanoparticles with a combination of compounds such as tartaric acid and ascorbic acid could be another strategy to overcome the agglomeration of iron oxide nanoparticles. However, due to low cytotoxicity displayed by such nanoparticles in Saos-2 cells, drug-loading of these nanoparticles should be considered for applications in osteosarcoma (Özel et al., 2019).

Gold Nanoparticles and 3D Printed Scaffolds

Gold Nanoparticles (AuNP) were incorporated into 3D printed gelatin methacrylate nanoparticles to enhance CT imaging (Celikkin et al., 2019). However, AuNPs have long been explored as anticancer tools. This is due to the outstanding properties of AuNPs such as multi-functionalization capabilities, high surface area to volume ratio, increased permeability, increased retention, stability, facile synthesis and surface chemistry (Singh et al., 2018). AuNPs are exogenous inducers of Reactive Oxygen Species (ROS). Cancer cells undergo apoptosis after exposure to AuNPS due to their inability to withstand the oxidative stress due to excess ROS generation (Dayem et al., 2017). It is important to note that cellular response to AuNPs differs across cell lines (Ju et al., 2015). The shape of AuNPs influences its cytotoxicity and anticancer potential. In one study, AuNP stars were proven to have greater cytotoxicity and anticancer potential than AuNP rods, while AuNP rods have greater cytotoxicity than AuNP spheres. This study was conducted employing a variety of cell lines including osteosarcoma cell lines (143-B, MG-63) (Steckiewicz et al., 2019). The size of AuNPs also influences its cytotoxicity. The larger the size of the AuNPs, the greater the cytotoxicity the AuNPs display. In one study, it was observed that 60 and 46 nm AuNPs displayed greater cytotoxicity than 38 nm AuNPs in MG-63 cells (Chakraborty et al., 2020).

AuNPs enhance the potency of drugs in osteosarcoma. Studies conducted have concluded that the effects of chemotherapeutics such as Doxorubicin (Iram et al., 2017; Steckiewicz et al., 2020), Cisplatin (Iram et al., 2017), bile acid cisplatin derivatives (Sánchez-Paradinas et al., 2014), Gemcitabine and Cytarabine

(Steckiewicz et al., 2020) are enhanced in osteosarcoma cell lines when conjugated to AuNPs. Glycogenic AuNPs have also proven to have anticancer potential (Rahim et al., 2014).

Silver Nanoparticles and 3D Printed Scaffolds

Silver nanoparticles (AgNP) are under intense investigation due to their remarkable physical, chemical and biological properties (Lee and Jun, 2019). AgNPs have been incorporated into 3D printed β-TCP scaffolds in the form of Ag-GO nanocomposites. First β-TCP scaffolds were fabricated followed by immersion in an Ag-GO suspension. The scaffolds displayed osteogenic and antibacterial activity (Zhang et al., 2017). However, AgNPs may also be incorporated into 3D scaffolds for anti-osteosarcoma applications. The ability of AgNP to induce apoptosis in cancer cells may be due to its ability to generate ROS which in turn leads to mitochondrial dysfunction (Dayem et al., 2017). Dávid Kovács et al. demonstrated that AgNP can induce apoptosis in osteosarcoma cells with and without the P53 tumor suppressor gene. Their results also proved that, unlike AuNPs, smaller AgNPs (5 nm) exhibited greater cytotoxicity than larger AgNPs (35 nm) (Kovács et al., 2016). The shape of AgNPs, unlike AuNPs, may not have an impact on cytotoxicity. In one study, no cell viability differences were noted between synthesized protein capped prism and spherical shaped AgNPs. By capping the AgNPs with proteins, the influence of AgNP shape on AgNP cytotoxicity could be analyzed without the complication of toxicity due to the surface chemistry of AgNP (Chakraborty et al., 2018). However, this study was conducted with Human cervical adenocarcinoma cells (HeLa cells) thus leaving a gap for exploration on the effects of different AgNP geometries in osteosarcoma cells.

The cytotoxicity of AgNPs may be enhanced in osteosarcoma cells by capping AgNPs with various agents such as adenosine 5′-triphosphate (ATP) (Rajabnia and Meshkini, 2018) and bovine serum albumin (Majeed et al., 2019). This was not the case, however, when AgNPs etched onto silica nanoparticles were functionalized with lipoic acid. Greater cytotoxicity in MG-63 osteosarcoma cells were found with plain AgNPs etched onto silica nanoparticles than those that were functionalized with lipoic acid (Tudose et al., 2017).

NANOCARRIERS FOR POTENTIAL INCORPORATION INTO 3D-PRINTED SCAFFOLDS

To the Author's knowledge, these nanoparticles have not yet been incorporated into scaffolds employed for bone regeneration. However, these nanoparticles are worth being mentioned, as their advancements in anti-osteosarcoma treatment may have the potential to be incorporated into scaffolds for localized adjuvant therapy.

Mesoporous Silica Nanoparticles as Anti-Osteosarcoma Nanocarriers

Mesoporous silica nanoparticles (MSNs) are inorganic nanoparticles that possess desirable attributes such as high surface area, tunable pore size, increased chemical, colloidal and thermal stability. In addition, their surfaces are easily modified (Murugan and Krishnan, 2018). MSNs are often capped with a gate-keeper that prevents premature release of loaded drug and can provide for controlled release of the contained drug (Murugan and Krishnan, 2018; Sábio et al., 2019).

MSNs have been widely explored as potential drug delivery vehicles. In the context of osteosarcoma, Martinez-Carmona et al. developed doxorubicin loaded MSNs by assembly of two different building blocks. The first building bock was a polyacrylic acid cap that was anchored to the MSNs by means of an acid cleavable acetal linker. This conferred a pH-responsive property. The second building block was the plant lectin concanavalin A which conferred a targeting property. These building blocks had a synergistic effect and potentiated the antitumor efficacy (Martínez-carmona et al., 2018). Paris et al. developed ultrasound responsive MSNs capped with polyethylene glycol (PEG). On exposure to ultrasound, the PEG capping was shed, resulting in the exposure of a cationic surface that enhanced osteosarcoma cell uptake of the MSNs that contained topotecan. The use of ultrasound increased the toxicity of the topotecan loaded MSNs (Paris et al., 2018). Lu et al. synthesized multifunctional mesoporous silica–coated bismuth sulfide nanoparticles that could treat osteosarcoma and facilitate Computed Tomography (CT) imaging. These nanoparticles were conjugated with the targeting peptide RGD and encapsulated doxorubicin. In addition, these nanoparticles have displayed potential for applications in photothermal therapy (Lu et al., 2018).

MSNs have also been explored as vectors for gene delivery in osteosarcoma. Xiong et al. synthesized magnetic core-shell MSNs with large radial mesopores. The MSNs were loaded with siRNA and were capped with tannic acid that served as a pH responsive gatekeeper (Xiong et al., 2016).

Dual drug delivery systems for application in osteosarcoma may prove to be advantageous, as they provide an opportunity to address the need for delivery of an antibacterial drug and an anticancer drug. Cheng et al. developed asymmetric, lollipop-shaped, dual compartment MSNs for co-delivery of hydrophobic and hydrophilic drugs. The MSN nanosphere head included iron oxide (Fe_3O_4) and enclosed the hydrophilic drug gentamicin. The "stick" of the lollipop was a nanorod of ethane bridged periodic mesoporous organosilica, and contained the hydrophobic drug curcumin. The asymmetrical MSNs displayed high antibacterial and high anticancer performance and can be used to load increased amounts of hydrophilic drugs (Cheng et al., 2020). This study was conducted using MCF-7 cells (human breast cancer cells).

One of the drawbacks of MSNs is its low biodegradability. A suggested strategy to tune the biodegradability of MSNs, is to dope MSNs with metal cations, such as zirconium, calcium, iron, and manganese. This has yet to be properly researched in the context of osteosarcoma (Croissant et al., 2017).

Micelles as Anti-Osteosarcoma Nanocarriers

Micelles are polymeric drug delivery vehicles assembled into a hydrophobic core/hydrophilic shell structure. As micellar shape and size are controllable, the drug loading capacity of micelles can be increased. The hydrophobic core of micelles allows the encapsulation of poorly soluble drugs, while the hydrophilic shell provides an opportunity for surface modification of the micelles to improve targeting (Melim et al., 2020).

In osteosarcoma, there exists several studies employing micelles as drug delivery systems to improve the therapeutic efficacy of hydrophobic drugs. Xi et al. loaded the compound curcumin into hyaluronic acid-octadecanoic acid micelles. These micelles were modified with alendronate to improve bone targeting. These micelles displayed high drug loading, high affinity to hydroxyapatite and sustained release (Xi et al., 2019). PEG-sheddable reduction-sensitive polyurethane micelles loaded with Doxorubicin were researched and was found to achieve triggered release. These micelles can also improve the antitumor efficacy of doxorubicin (Yang et al., 2020). Fang et al. developed micelles formed from poly (ethylene glycol)-block-poly (trimethylene carbonate) terminated with the cell affinitive peptide RGD. These RGD terminate micelles displayed increased cell uptake as compared to micelles not terminated with RGD (Fang et al., 2017).

Micelles could also be used to deliver hydrophilic drugs in osteosarcoma. Noy et al. reported the incorporation of PENAO (an arsenic drug-(4-(N-(S-penicillaminylacetyl) amino)) into the micelle polymer matrix. This prevents drug leakage and premature release of PENAO (Noy et al., 2018). Noy et al. also noted that due to the minimal availability of hydrophilic drugs, there is little information on the effect of hydrophilic drugs on the micelle surfaces (Noy et al., 2018). More research should be conducted on such effects.

Micelles may be stable in aqueous solutions, however when immersed in blood, dissociation occurs, leading to accelerated drug release (Li et al., 2014). Therefore, strategies such as cross-linking the micelle core has been developed to improve micelle stability in the blood (Cajot et al., 2011). However, cross-linking the core of the micelle may decrease the drug loading capacity, therefore, other methods such as interface crosslinking may be more suitable (Lu et al., 2020).

Targeted Nanocarriers and Stimuli-Responsive Nanocarriers

Should a nanocarrier-loaded scaffold be employed for bone regeneration and adjuvant therapy after osteosarcoma resection, targeting strategies and intrinsic stimuli-responsive nanocarriers (such as pH and redox responsive nanocarriers) should be considered, to provide chemotherapeutic delivery that is specific to cancer cells.

Drug delivery may be controlled by utilising the pH gradients present between normal physiological compartment and tumor tissue. The normal physiological pH of blood is 7.4, while the pH of the extracellular tumor tissue is more acidic at 6.0–7.2. The pH of subcellular compartments have a lower pH compared to the extracellular environment- the lysosome has pH of between 4.0–5.0 while endosomes have a pH of 5.0–6.0 (Bertrand et al., 2014; Ruttala et al., 2018). pH-responsive nanocarriers may developed by use of two means: i) the nanocarrier is formed from, capped or layered with a pH-responsive polymer (e.g. chitosan) or ii) there are pH-sensitive moieties employed to link either a drug or polymer to the nanocarrier (e.g. hydrazone and acetal bonds) (Lavrador et al., 2018; Ruttala et al., 2018). **Table 1** details the types of pH-responsive nanoparticles explored in osteosarcoma and what confers the pH-responsive characteristic to the nanoparticle.

Glutathione is a tripeptide (cysteine, glycine, and glutamic acid) and is found abundantly in the mammalian cell with an abundance of important functions. Glutathione in its reduced state exists as GSH (Pizzorno, 2014). GSH is present in intracellular environments in concentrations that are approximately 100 times greater than the GSH concentrations present in the extracellular environment (Lavrador et al., 2018; Ruttala et al., 2018). A study revealed that intrinsic GSH concentrations correlated to cisplatin resistance in osteosarcoma cells and that a depletion of GSH increased the sensitivity of osteosarcoma cells to cisplatin (Komiya et al., 1998). The redox potential created by the difference of glutathione levels between the intracellular and extracellular environments provides an opportunity for a stimuli-responsive mechanism. By adding a disulfide linkage to the nanocarrier, drugs may be released in the intracellular environment where GSH concentrations are increased (Lavrador et al., 2018; Ruttala et al., 2018). **Table 1** also demonstrates the redox nanocarriers synthesized for use in osteosarcoma.

Targeting may be classified into active and passive targeting. To enhance active targeting, functionalizing nanoparticles with ligands that lead to surface interaction with overexpressed surface molecule and proteins on cancer cells, thereby facilitating cellular uptake via receptor-mediated endocytosis (Huang et al., 2020). **Figure 5** illustrates the internalization of nanocarriers by the cell through receptor-mediated endocytosis by use of a targeting ligand. **Table 3** discusses the targeting strategies that have been employed in nanoparticles for osteosarcoma treatment. **Table 4** describes the strategies that have been researched in imbuing nanocarriers with intrinsic stimuli-responsive properties.

DISCUSSION

In this literature review, the various polymers and bioceramics utilized for 3D printed scaffolds as well as the nanocarriers that may be incorporated into these scaffolds that may be employed for bone tissue engineering has been discussed. For these scaffolds to be utilized for application in post-surgical resection of osteosarcoma however, certain factors have to be taken into account. Scaffolds that have mechanical strength only suitable for non-load bearing joints may not be utilized for application in post-surgical resections of osteosarcoma of load-bearing bones. Based on the data presented, there is much research to be done on

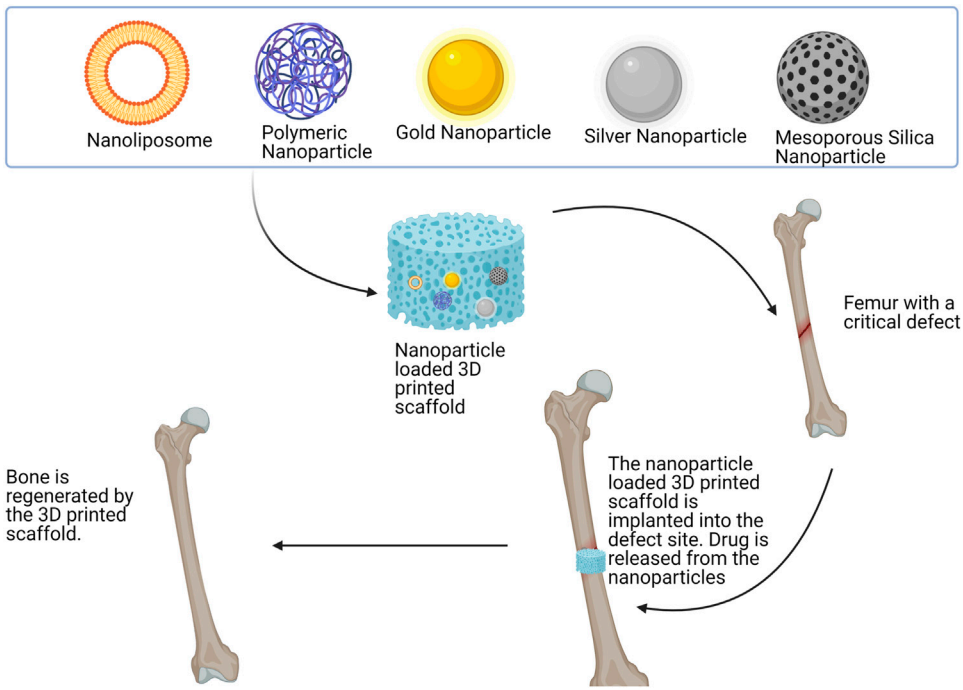

FIGURE 5 | The various types of nanocarriers that may be incorporated into a scaffold. The nanocarriers are included in a 3D printed scaffold. The scaffold is then implanted into the critical defect site present in the femur due to osteosarcoma resection. Chemotherapeutics are released from the scaffold to target residual cancer cells while the scaffold regenerates the bone. This figure was created with BioRender.com.

TABLE 3 | Information on strategies to confer targeting properties to nanoparticles.

Target	Nanoparticle	Drug	Compound that conferred targeting properties	References
Bone targeting	Polymeric nanoparticle	Paclitaxel	Alendronate (bisphosphonate)	Zhao et al. (2019)
Bone (hydroxyapatite) and CD44	Liposome	Doxorubicin	Alendronate and hyaluronic acid	Feng S. et al. (2019)
Bone targeting (hydroxyapatite)	Micelle	Doxorubicin	D-aspartic acid octapeptide	Low et al. (2014)
CD44	Liposome	Doxorubicin conjugated with a H2S-releasing moiety	Hyaluronic acid	Gazzano et al. (2019)
CD44	Liposome	Doxorubicin	Hyaluronic acid	Chi et al. (2017)
CD44 Hydroxyapatite	Micelle	Curcumin	Hyaluronic acid Alendronate	Xi et al. (2019)
CD133	Lipid-polymeric nanoparticle	All-trans retinoic acid	CD133 aptamers	Gui et al. (2019)
EphA2 receptor	Liposome	Doxorubicin and siRNA	YSA peptide	Haghiralsadat et al. (2018)
Epidermal growth factor CD133	Lipid-polymeric nanoparticle	Salinomycin	EGFR and CD133 aptamers	Chen F. et al. (2018)
Epidermal growth factor	Lipid-polymer nanoparticle	Salinomycin	EGFR aptamer	Yu et al. (2018)
Estrogen receptors	Liposome	Doxorubicin	Estrogen	Yin et al. (2018)
Integrin receptors—αvβ3 and αvβ5	MSN	Doxorubicin	Targeting peptide RGD	Lu et al. (2018)
Integrin receptors—αvβ3 and αvβ5	Micelle	Doxorubicin	RGD	Fang et al. (2017)
Over expressed cell surface glycans	MSN	Doxorubicin	Lectin concanavalin A	Martínez-carmona et al. (2018)
Overexpressed folate receptors	Mesoporous zinc-substituted hydroxyapatite	Methotrexate	Methotrexate	Meshkini and Oveisi, (2017)

TABLE 4 | Information on strategies utilized to confer intrinsic stimuli properties to nanoparticles as well as the anti-osteosarcoma drugs and cell lines utilized.

Intrinsic stimuli	Nanoparticle	Anti-osteosarcoma drug/compound	Compound that conferred stimuli responsive property	OS cell line	References
pH	MSN	Doxorubicin	Poly acrylic acid cap linked by acetal cleavable linker	HOS cells- CRL-1543 Mouse preosteoblastic cell line -MC3T3-E1	Martínez-carmona et al. (2018)
	MSN	siRNA	Tannic acid	KHOS	Xiong et al. (2016)
	Calcium carbonate ($CaCO_3$)-based therapeutic modulator with a layer of Collagen type I	CeO_2 and doxorubicin	$CaCO_3$	Saos-2	Tapeinos et al. (2018)
	Liposome	Doxorubicin	Cationic nitrogen of the ammonium moiety	Mouse osteosarcoma cells (K7M2)	Rayamajhi et al. (2020)
	Micelle	Doxorubicin	Hydrazone bond that bound Doxorubicin	Saos-2	Low et al. (2014)
	Cationic cyclodextrin coated magnetic nanoparticles	Methotrexate	Ionic interaction between carboxylate anions of methotrexate and the nanocarrier	Saos-2	Ahmadi et al. (2020)
	Mesoporous ZSM-5 zeolites	Doxorubicin	Chitosan layer	MG-63	Yang et al. (2018)
Redox	Liposome (estrogen functionalized)	Doxorubicin	The disulfate bond that tethered the chitooligosaccharides to the liposome	MG-63	Yin et al. (2018)
	Liposome	Doxorubicin	The disulfide linker that attached the chitooligosaccharide to cholesterol	MG-63	Yin et al. (2017)
	Liposome	Doxorubicin	Disulfide bonds that linked PEG with cholesterol	MG-63	Chi et al. (2017)
	Liposome (dual targeting-bone and CD44)	Doxorubicin	Disulfide bond that links Alendronate-hyaluronic acid to PEG_{2000}–DSPE	MG-63	Feng S. et al. (2019)
	Micelle	Doxorubicin	Disulfide bonds attached to PEG. Disulfide bonds attached to polyurethane	Saos-2	Yang et al. (2020)

3D printing polymeric scaffolds for bone regeneration at loadbearing sites. The ideal combination of polymers to fabricate 3D printed scaffolds for bone regeneration has yet to be established.

Other 3D printed scaffolds that require further research as potential scaffolds for bone regeneration are 3D printed nanoclay composite scaffolds. Coppola et al. (2018) investigated the influence of temperature on PLA/clay nanocomposites. The nanoclay used was Cloisite 30B modified by methyl, tallow, bis-2-hydroxyethyl, and quaternary ammonium chloride. The samples were printed by FDM and two PLA grades were used. It was concluded that PLA nanocomposite samples had a higher elastic modulus that plain PLA samples. PLA nanocomposite with D-isomer at 4 displayed an increase in elastic modulus as the printing temperature increased. Other noteworthy observations include that nanoclay acted as a nucleating agent and increased thermal stability (Coppola et al., 2018). However, cell studies should be conducted on these scaffolds to determine their suitability for bone regeneration. Cidonio et al. also used Laponite (a type of nanoclay) for its physiochemical and osteogenic differentiation inducing properties in a bioink that also consisted of alginate and methyl cellulose. These scaffolds were fabricated with their own in-house 3D printer. Based on *in vitro, ex vivo and in vitro* studies it was concluded that scaffolds produced from the nanoclay-based bioink had the potential to be clinically relevant bone regenerative constructs (Cidonio et al., 2020). Further investigation and research should include the formulation of polymer/bioceramic/nanoclay as well as various other polymer/nanoclay 3D printed scaffolds for the suitability of bone regeneration in the context of osteosarcoma.

One of the drawbacks to 3D printing is that the materials used in the direct printing of scaffolds may be limited due to the printing technology available. Indirect 3D printing approaches may be undertaken to overcome drawbacks of 3D printing such as 3D printing a dissolvable negative mold to cast the solutions required for the scaffolds. The 3D printed mold can then be dissolved once the scaffold has set by methods such as lyophilization (Sachlos et al., 2006; Hassanajili et al., 2019).

The bone regeneration abilities of polymers in bone tissue engineering may be enhanced by incorporating other compounds, molecules and drugs such as BMP and VEGF. Photo- responsive and magneto-responsive 3D printed scaffolds may be utilized for applications in post-surgical-resection of osteosarcoma. However, due to poor penetration of NIR through tissue, other routes to facilitate NIR reaching the scaffolds must be considered.

Recent studies indicate that bone regeneration abilities of polymers may also be enhanced by the inclusion of Magnesium (Mg). Golafshan et al. (2020) prepared Magnesium Phosphate scaffolds modified with Strontium ions (MPSr) by including it in a polymer phase. The polymer selected was polycaprolactone. Scaffolds with 30 wt% of PCL could print the desired shape by extrusion-based printing. It was concluded that when compared to pristine PCL scaffolds, MPSr/PCL scaffolds were superior in terms of biological and mechanical qualities (Golafshan et al., 2020). Lai et al. (2019) developed 3D printed poly (lactide-co-glycolide) (PLGA)/β-TCP/Mg scaffolds by utilising low-temperature rapid prototyping. PLGA/β-TCP/Mg scaffolds displayed osteogenic and angiogenic properties. *In vivo* studies further demonstrated that subjects with PLGA/

β-TCP/Mg scaffolds had greater mean bone volume than those with just PLGA/β-TCP scaffolds (Lai et al., 2019). Thus, incorporating Mg into other 3D printed polymeric/bioceramic scaffolds should be considered for future studies that research 3D printed scaffolds for application in osteosarcoma.

In conclusion, 3D printed scaffolds pose an opportunity with untapped potential. They may be used as sustained release platforms for drugs not just to enhance bone regeneration, but to target residual osteosarcoma cells after surgical resection and to mitigate infections after surgical implantation of the scaffold. This may be achieved by two means so far; to directly load the drug within the scaffold (if the drug is suitable) or to load the scaffolds with drug encapsulated nanoparticles which can overcome limitations such as poor solubility and toxicity that are inherent to many drugs. Strategies such as tagging the nanocarriers with targeting compounds and refining nanocarriers to respond to certain stimuli may allow for precision in targeting cancer cells in adjuvant therapy.

AUTHOR CONTRIBUTIONS

All authors listed have made a substantial, direct, and intellectual contribution to the work and approved it for publication.

FUNDING

The financial assistance of the National Research Foundation (NRF) towards this research is hereby acknowledged. Opinions expressed and conclusions arrived at, are those of the author and are not necessarily to be attributed to the NRF.

ACKNOWLEDGMENTS

Professor Viness Pillay, who passed away on July 24, 2020, is hereby kindly acknowledged and remembered for his contributions in this field of research.

REFERENCES

Abbasi, N., Hamlet, S., Love, R. M., and Nguyen, N.-T. (2020). Porous Scaffolds for Bone Regeneration. *J. Sci. Adv. Mater. Devices* 5, 1–9. doi:10.1016/j.jsamd.2020.01.007

Ahmadi, D., Zarei, M., Rahimi, M., Khazaie, M., Asemi, Z., Mir, S. M., et al. (2020). Preparation and Iin-Vvitro Evaluation of pH-Responsive Cationic Cyclodextrin Coated Magnetic Nanoparticles for Delivery of Methotrexate to the Saos-2 Bone Cancer Cells. *J. Drug Deliv. Sci. Techn.* 57, 101584. doi:10.1016/j.jddst.2020.101584

Ahmed, S., Ahmad, M., Jayachandran, M., Qureshi, M. A., and Ikram, S. (2015). Chitosan Based Dressings for Wound Care. *Immunochem. Immunopathol. Open Access* 1, 1–6. doi:10.4172/icoa.1000106

Alavi, M., and Hamidi, M. (2019). Passive and Active Targeting in Cancer Therapy by Liposomes and Lipid Nanoparticles. *Drug Metab. Pers. Ther.* 34, 1–8. doi:10.1515/dmpt-2018-0032

Alksne, M., Kalvaityte, M., Simoliunas, E., Rinkunaite, I., Gendviliene, I., Locs, J., et al. (2020). *In Vitro* comparison of 3D Printed Polylactic Acid/hydroxyapatite and Polylactic Acid/bioglass Composite Scaffolds: Insights into Materials for Bone Regeneration. *J. Mech. Behav. Biomed. Mater.* 104, 103641. doi:10.1016/j.jmbbm.2020.103641

Anbu, R. T., Suresh, V., Gounder, R., and Kannan, A. (2019). Comparison of the Efficacy of Three Different Bone Regeneration Materials: An Animal Study. *Eur. J. Dent.* 13, 022–028. doi:10.1055/s-0039-1688735

Andersson, H., Kim, Y.-S., O'Neill, B., Shi, Z.-Z., and Serda, R. (2014). HSP70 Promoter-Driven Activation of Gene Expression for Immunotherapy Using Gold Nanorods and Near Infrared Light. *Vaccines* 2, 216–227. doi:10.3390/vaccines2020216

Bai, J., Wang, H., Gao, W., Liang, F., Wang, Z., Zhou, Y., et al. (2020). Melt Electrohydrodynamic 3D Printed Poly (ε-Caprolactone)/polyethylene Glycol/roxithromycin Scaffold as a Potential Anti-infective Implant in Bone Repair. *Int. J. Pharmaceutics* 576, 118941. doi:10.1016/j.ijpharm.2019.118941

Baino, F. (2018). Bioactive Glasses - when Glass Science and Technology Meet Regenerative Medicine. *Ceramics Int.* 44, 14953–14966. doi:10.1016/j.ceramint.2018.05.180

Bendtsen, S. T., Quinnell, S. P., and Wei, M. (2017). Development of a Novel Alginate-Polyvinyl Alcohol-Hydroxyapatite Hydrogel for 3D Bioprinting Bone Tissue Engineered Scaffolds. *J. Biomed. Mater. Res.* 105, 1457–1468. doi:10.1002/jbm.a.36036

Bertrand, N., Wu, J., Xu, X., Kamaly, N., and Farokhzad, O. C. (2014). Cancer Nanotechnology: The Impact of Passive and Active Targeting in the Era of Modern Cancer Biology. *Adv. Drug Deliv. Rev.* 66, 2–25. doi:10.1016/j.addr.2013.11.009

Bhattacharjee, P., Kundu, B., Naskar, D., Kim, H.-W., Maiti, T. K., Bhattacharya, D., et al. (2017). Silk Scaffolds in Bone Tissue Engineering: An Overview. *Acta Biomater.* 63, 1–17. doi:10.1016/j.actbio.2017.09.027

Bil, M., Ryszkowska, J., Woźniak, P., Kurzydłowski, K. J., and Lewandowska-Szumieł, M. (2010). Optimization of the Structure of Polyurethanes for Bone Tissue Engineering Applications. *Acta Biomater.*, 6, 2501–2510. doi:10.1016/j.actbio.2009.08.037

Boskey, A. (2003). Biomineralization: An Overview. *Connect. Tissue Res.* 44, 5–9. doi:10.1080/03008200390152007 10.1080/713713622

Bruyas, A., Lou, F., Stahl, A. M., Gardner, M., Maloney, W., Goodman, S., et al. (2018). Systematic Characterization of 3D-Printed PCL/β-TCP Scaffolds for Biomedical Devices and Bone Tissue Engineering: Influence of Composition and Porosity. *J. Mater. Res.* 33, 1948–1959. doi:10.1557/jmr.2018.112

Bulbake, U., Doppalapudi, S., Kommineni, N., and Khan, W. (2017). Liposomal Formulations in Clinical Use: An Updated Review. *Pharmaceutics*.9, 12. doi:10.3390/pharmaceutics9020012

Caballero, S. S. R., Saiz, E., Montembault, A., Tadier, S., Maire, E., David, L., et al. (2019). 3-D Printing of Chitosan-Calcium Phosphate Inks: Rheology, Interactions and Characterization. *J. Mater. Sci. Mater. Med.* 30, 6. doi:10.1007/s10856-018-6201-y

Cajot, S., Lautram, N., Passirani, C., and Jérôme, C. (2011). Design of Reversibly Core Cross-Linked Micelles Sensitive to Reductive Environment. *J. Controlled Release* 152, 30–36. doi:10.1016/j.jconrel.2011.03.026

Caliskan, Y., Dalgic, A. D., Gerekci, S., Gulec, E. A., Tezcaner, A., Ozen, C., et al. (2019). A New Therapeutic Combination for Osteosarcoma: Gemcitabine and Clofazimine Co-loaded Liposomal Formulation. *Int. J. Pharmaceutics* 557, 97–104. doi:10.1016/j.ijpharm.2018.12.041

Celikkin, N., Mastrogiacomo, S., Walboomers, X., and Swieszkowski, W. (2019). Enhancing X-ray Attenuation of 3D Printed Gelatin Methacrylate (GelMA) Hydrogels Utilizing Gold Nanoparticles for Bone Tissue Engineering Applications. *Polymers* 11, 367. doi:10.3390/POLYM11020367

Chakraborty, A., Das, A., Raha, S., and Barui, A. (2020). Size-dependent Apoptotic Activity of Gold Nanoparticles on Osteosarcoma Cells Correlated with SERS Signal. *J. Photochem. Photobiol. B: Biol.* 203, 111778. doi:10.1016/j.jphotobiol.2020.111778

Chakraborty, I., Feliu, N., Roy, S., Dawson, K., and Parak, W. J. (2018). Protein-Mediated Shape Control of Silver Nanoparticles. *Bioconjug. Chem.* 29, 1261–1265. doi:10.1021/acs.bioconjchem.8b00034

Chavanne, P., Stevanovic, S., Wüthrich, A., Braissant, O., Pieles, U., Gruner, P., et al. (2013). 3D Printed Chitosan/Hydroxyapatite Scaffolds for Potential Use in Regenerative Medicine. *Biomed. Tech.* 58, 2–3. doi:10.1515/bmt-2013-40

Chen, F., Zeng, Y., Qi, X., Chen, Y., Ge, Z., Jiang, Z., et al. (2018). Targeted Salinomycin Delivery with EGFR and CD133 Aptamers Based Dual-Ligand

Lipid-Polymer Nanoparticles to Both Osteosarcoma Cells and Cancer Stem Cells. *Nanomedicine: Nanotechnology, Biol. Med.* 14, 2115–2127. doi:10.1016/j.nano.2018.05.015

Chen, G., Chen, N., and Wang, Q. (2019). Fabrication and Properties of Poly(vinyl Alcohol)/β-Tricalcium Phosphate Composite Scaffolds via Fused Deposition Modeling for Bone Tissue Engineering. *Composites Sci. Techn.* 172, 17–28. doi:10.1016/j.compscitech.2019.01.004

Chen, S., Shi, Y., Zhang, X., and Ma, J. (2020). Evaluation of BMP-2 and VEGF Loaded 3D Printed Hydroxyapatite Composite Scaffolds with Enhanced Osteogenic Capacity *In Vitro* and *In Vivo*. *Mater. Sci. Eng. C* 112, 110893. doi:10.1016/j.msec.2020.110893

Chen, X., Fan, H., Deng, X., Wu, L., Yi, T., Gu, L., et al. (2018). Scaffold Structural Microenvironmental Cues to Guide Tissue Regeneration in Bone Tissue Applications. *Nanomaterials* 8, 960. doi:10.3390/nano8110960

Cheng, Y., Zhang, Y., Deng, W., and Hu, J. (2020). Antibacterial and Anticancer Activities of Asymmetric Lollipop-like Mesoporous Silica Nanoparticles Loaded with Curcumin and Gentamicin Sulfate. *Colloids Surf. B: Biointerfaces* 186, 110744. doi:10.1016/j.colsurfb.2019.110744

Chi, Y., Yin, X., Sun, K., Feng, S., Liu, J., Chen, D., et al. (2017). Redox-sensitive and Hyaluronic Acid Functionalized Liposomes for Cytoplasmic Drug Delivery to Osteosarcoma in Animal Models. *J. Controlled Release* 261, 113–125. doi:10.1016/j.jconrel.2017.06.027

Chiu, Y.-C., Shie, M.-Y., Lin, Y.-H., Lee, A. K.-X., and Chen, Y.-W. (2019). Effect of Strontium Substitution on the Physicochemical Properties and Bone Regeneration Potential of 3D Printed Calcium Silicate Scaffolds. *Int. J. Mol. Sci.* 20, 2729. doi:10.3390/ijms20112729

Chou, A. J., Geller, D. S., and Gorlick, R. (2008). Therapy for Osteosarcoma. *Pediatr. Drugs* 10, 315–327. doi:10.2165/00148581-200810050-00005

Choudhury, H., Gorain, B., Pandey, M., Khurana, R. K., and Kesharwani, P. (2019). Strategizing Biodegradable Polymeric Nanoparticles to Cross the Biological Barriers for Cancer Targeting. *Int. J. Pharmaceutics* 565, 509–522. doi:10.1016/j.ijpharm.2019.05.042

Cidonio, G., Glinka, M., Kim, Y.-H., Kanczler, J. M., Lanham, S. A., Ahlfeld, T., et al. (2020). Nanoclay-based 3D Printed Scaffolds Promote Vascular Ingrowth *Ex Vivo* and Generate Bone mineral Tissue *In Vitro* and *In Vivo*. *Biofabrication* 12, 035010. doi:10.1088/1758-5090/ab8753

Coppola, B., Cappetti, N., Di Maio, L., Scarfato, P., and Incarnato, L. (2018). 3D Printing of PLA/clay Nanocomposites: Influence of Printing Temperature on Printed Samples Properties. *Materials* 11, 1947. doi:10.3390/ma11101947

Croissant, J. G., Fatieiev, Y., and Khashab, N. M. (2017). Degradability and Clearance of Silicon, Organosilica, Silsesquioxane, Silica Mixed Oxide, and Mesoporous Silica Nanoparticles. *Adv. Mater.*, 29, 1604634. doi:10.1002/adma.201604634

Dang, W., Li, T., Li, B., Ma, H., Zhai, D., Wang, X., et al. (2018). A Bifunctional Scaffold with CuFeSe2 Nanocrystals for Tumor Therapy and Bone Reconstruction. *Biomaterials* 160, 92–106. doi:10.1016/j.biomaterials.2017.11.020

Datta, A., Ghosh, A. K., and Kundu, S. C. (2001). Differential Expression of the Fibroin Gene in Developmental Stages of Silkworm, Antheraea Mylitta (Saturniidae). *Comp. Biochem. Physiol. B: Biochem. Mol. Biol.* 129, 197–204. doi:10.1016/S1096-4959(01)00377-3

Dayem, A. A., Hossain, M. K., Lee, S. B., Kim, K., Saha, S. K., Yang, G., et al. (2017). The Role of Reactive Oxygen Species (ROS) in the Biological Activities of Metallic Nanoparticles. *Int. J. Mol. Sci.* 18, 120. doi:10.3390/ijms18010120

Demirtaş, T. T., Irmak, G., and Gümüşderelioğlu, M. (2017). A Bioprintable Form of Chitosan Hydrogel for Bone Tissue Engineering. *Biofabrication* 9, 035003. doi:10.1088/1758-5090/aa7b1d

Djagny, K. B., Wang, Z., and Xu, S. (2001). Gelatin: A Valuable Protein for Food and Pharmaceutical Industries: Review. *Crit. Rev. Food Sci. Nutr.* 41, 481–492. doi:10.1080/20014091091904

Du, S., Li, J., Du, C., Huang, Z., Chen, G., and Yan, W. (2017). Overendocytosis of Superparamagnetic Iron Oxide Particles Increases Apoptosis and Triggers Autophagic Cell Death in Human Osteosarcoma Cell under a Spinning Magnetic Field. *Oncotarget* 8, 9410–9424. doi:10.18632/oncotarget.14114

Du, X., Wei, D., Huang, L., Zhu, M., Zhang, Y., and Zhu, Y. (2019). 3D Printing of Mesoporous Bioactive Glass/silk Fibroin Composite Scaffolds for Bone Tissue Engineering. *Mater. Sci. Eng. C* 103, 109731. doi:10.1016/j.msec.2019.05.016

Duan, R., Li, C., Wang, F., and Yangi, J.-C. (2017). Polymer-lipid Hybrid Nanoparticles-Based Paclitaxel and Etoposide Combinations for the Synergistic Anticancer Efficacy in Osteosarcoma. *Colloids Surf. B: Biointerfaces* 159, 880–887. doi:10.1016/j.colsurfb.2017.08.042

Dwivedi, R., Kumar, S., Pandey, R., Mahajan, A., Nandana, D., Katti, D. S., et al. (2020). Polycaprolactone as Biomaterial for Bone Scaffolds: Review of Literature. *J. Oral Biol. Craniofac. Res.* 10, 381–388. doi:10.1016/j.jobcr.2019.10.003

Echave, M. C., Sánchez, P., Pedraz, J. L., and Orive, G. (2017). Progress of Gelatin-Based 3D Approaches for Bone Regeneration. *J. Drug Deliv. Sci. Techn.* 42, 63–74. doi:10.1016/j.jddst.2017.04.012

Ergul, N. M., Unal, S., Kartal, I., Kalkandelen, C., Ekren, N., Kilic, O., et al. (2019). 3D Printing of Chitosan/Poly(vinyl Alcohol) Hydrogel Containing Synthesized Hydroxyapatite Scaffolds for Hard-Tissue Engineering. *Polym. Test.* 79, 106006. doi:10.1016/j.polymertesting.2019.106006

Fahimipour, F., Rasoulianboroujeni, M., Dashtimoghadam, E., Khoshroo, K., Tahriri, M., Bastami, F., et al. (2017). 3D Printed TCP-Based Scaffold Incorporating VEGF-Loaded PLGA Microspheres for Craniofacial Tissue Engineering. *Dental Mater.* 33, 1205–1216. doi:10.1016/j.dental.2017.06.016

Fang, Z., Sun, Y., Xiao, H., Li, P., Liu, M., Ding, F., et al. (2017). Targeted Osteosarcoma Chemotherapy Using RGD Peptide-Installed Doxorubicin-Loaded Biodegradable Polymeric Micelle. *Biomed. Pharmacother.* 85, 160–168. doi:10.1016/j.biopha.2016.11.132

Feng, P., Jia, J., Peng, S., Yang, W., Bin, S., and Shuai, C. (2020). Graphene Oxide-Driven Interfacial Coupling in Laser 3D Printed PEEK/PVA Scaffolds for Bone Regeneration. *Virtual Phys. Prototyping* 15, 211–226. doi:10.1080/17452759.2020.1719457

Feng, S., Wu, Z.-X., Zhao, Z., Liu, J., Sun, K., Guo, C., et al. (2019). Engineering of Bone- and CD44-Dual-Targeting Redox-Sensitive Liposomes for the Treatment of Orthotopic Osteosarcoma. *ACS Appl. Mater. Inter.* 11, 7357–7368. doi:10.1021/acsami.8b18820

Feng, X., Wu, Y., Bao, F., Chen, X., and Gong, J. (2019). Comparison of 3D-Printed Mesoporous Calcium Silicate/polycaprolactone and Mesoporous Bioacive Glass/polycaprolactone Scaffolds for Bone Regeneration. *Microporous Mesoporous Mater.* 278, 348–353. doi:10.1016/j.micromeso.2019.01.007

Ferreira, A. M., Gentile, P., Chiono, V., and Ciardelli, G. (2012). Collagen for Bone Tissue Regeneration. *Acta Biomater.* 8, 3191–3200. doi:10.1016/j.actbio.2012.06.014

Fu, S., Hu, H., Chen, J., Zhu, Y., and Zhao, S. (2020). Silicone Resin Derived Larnite/C Scaffolds via 3D Printing for Potential Tumor Therapy and Bone Regeneration. *Chem. Eng. J.* 382, 122928. doi:10.1016/j.cej.2019.122928

Gazzano, E., Buondonno, I., Marengo, A., Rolando, B., Chegaev, K., Kopecka, J., et al. (2019). Hyaluronated Liposomes Containing H2S-Releasing Doxorubicin Are Effective against P-Glycoprotein-Positive/doxorubicin-Resistant Osteosarcoma Cells and Xenografts. *Cancer Lett.* 456, 29–39. doi:10.1016/j.canlet.2019.04.029

Ghorbani, F., Li, D., Ni, S., Zhou, Y., and Yu, B. (2020). 3D Printing of Acellular Scaffolds for Bone Defect Regeneration:. *A Review. Mater. Today Commun.* 22, 100979. doi:10.1016/j.mtcomm.2020.100979

Giannoudis, P. V., Einhorn, T. A., and Marsh, D. (2007). Fracture Healing: The diamond Concept. *Injury* 38, S3–S6. doi:10.1016/s0020-1383(08)70003-2

Giannoudis, P. V., Einhorn, T. A., Schmidmaier, G., and Marsh, D. (2008). The diamond Concept - Open Questions. *Injury* 39, S5–S8. doi:10.1016/S0020-1383(08)70010-X

Giansanti, L., Condello, M., Altieri, B., Galantini, L., Meschini, S., and Mancini, G. (2019). Influence of Lipid Composition on the Ability of Liposome Loaded Voacamine to Improve the Reversion of Doxorubicin Resistant Osteosarcoma Cells. *Chem. Phys. Lipids* 223, 104781. doi:10.1016/j.chemphyslip.2019.05.006

Golafshan, N., Vorndran, E., Zaharievski, S., Brommer, H., Kadumudi, F. B., Dolatshahi-Pirouz, A., et al. (2020). Tough Magnesium Phosphate-Based 3D-Printed Implants Induce Bone Regeneration in an Equine Defect Model. *Biomaterials* 261, 120302. doi:10.1016/j.biomaterials.2020.120302

Gómez-Cerezo, M. N., Lozano, D., Arcos, D., Vallet-Regí, M., and Vaquette, C. (2020). The Effect of Biomimetic Mineralization of 3D-Printed Mesoporous Bioglass Scaffolds on Physical Properties and *In Vitro* Osteogenicity. *Mater. Sci. Eng. C* 109, 110572. doi:10.1016/j.msec.2019.110572

Gui, K., Zhang, X., Chen, F., Ge, Z., Zhang, S., Qi, X., et al. (2019). Lipid-polymer Nanoparticles with CD133 Aptamers for Targeted Delivery of All-Trans

Retinoic Acid to Osteosarcoma Initiating Cells. *Biomed. Pharmacother.* 111, 751–764. doi:10.1016/j.biopha.2018.11.118

Haghiralsadat, F., Amoabediny, G., Naderinezhad, S., Zandieh-Doulabi, B., Forouzanfar, T., and Helder, M. N. (2018). Codelivery of Doxorubicin and JIP1 siRNA with Novel EphA2-Targeted Pegylated Cationic Nanoliposomes to Overcome Osteosarcoma Multidrug Resistance. *Int. J. Nanomedicine.* Vol. 13, 3853–3866. doi:10.2147/IJN.S150017

Hassanajili, S., Karami-Pour, A., Oryan, A., and Talaei-Khozani, T. (2019). Preparation and Characterization of PLA/PCL/HA Composite Scaffolds Using Indirect 3D Printing for Bone Tissue Engineering. *Mater. Sci. Eng. C* 104, 109960. doi:10.1016/j.msec.2019.109960

Heck, R. K., and Toy, P. C. (2017). "Malignant Tumors of Bone," in *Campbell's Operative Orthopaedics*. Philadelphia: Elsevier, 945–983. Available at: https://www.clinicalkey.com/#!/content/book/3-s2.0-B9780323374620000276?scrollTo=%23hl0000691.

Henderson, T. A., and Morries, L. (2015). Near-infrared Photonic Energy Penetration: Can Infrared Phototherapy Effectively Reach the Human Brain? *Neurophyschiatr. Des. Treat.* 11, 2191–2208. doi:10.2147/NDT.S78182

Heo, E. Y., Ko, N. R., Bae, M. S., Lee, S. J., Choi, B.-J., Kim, J. H., et al. (2017). Novel 3D Printed Alginate-BFP1 Hybrid Scaffolds for Enhanced Bone Regeneration. *J. Ind. Eng. Chem.* 45, 61–67. doi:10.1016/j.jiec.2016.09.003

Heo, S. Y., Ko, S. C., Oh, G. W., Kim, N., Choi, I. W., Park, W. S., et al. (2019). Fabrication and Characterization of the 3D-Printed Polycaprolactone/fish Bone Extract Scaffolds for Bone Tissue Regeneration. *J. Biomed. Mater. Res.* 107, 1937–1944. doi:10.1002/jbm.b.34286

Hernandez, I., Kumar, A., and Joddar, B. (2017). A Bioactive Hydrogel and 3D Printed Polycaprolactone System for Bone Tissue Engineering. *Gels* 3, 26. doi:10.3390/gels3030026

Hernández-González, A. C., Téllez-Jurado, L., and Rodríguez-Lorenzo, L. M. (2020). Alginate Hydrogels for Bone Tissue Engineering, from Injectables to Bioprinting: A Review. *Carbohydr. Polym.* 229, 115514. doi:10.1016/j.carbpol.2019.115514

Hoque, M., Nuge, T., Yeow, T., Nordin, N., and Prasad, R. (2015). Gelatin Based Scaffolds for Tissue Engineering-A Review. *Polym. Res. J.* 9, 15.

Huang, Q.-w., Wang, L.-p., and Wang, J.-y. (2014). Mechanical Properties of Artificial Materials for Bone Repair. *J. Shanghai Jiaotong Univ. (Sci.)* 19, 675–680. doi:10.1007/s12204-014-1565-8

Huang, T., Fan, C., Zhu, M., Zhu, Y., Zhang, W., and Li, L. (2019). 3D-printed Scaffolds of Biomineralized Hydroxyapatite Nanocomposite on Silk Fibroin for Improving Bone Regeneration. *Appl. Surf. Sci.* 467-468, 345–353. doi:10.1016/j.apsusc.2018.10.166

Huang, X., Wu, W., Yang, W., Qing, X., and Shao, Z. (2020). Surface Engineering of Nanoparticles with Ligands for Targeted Delivery to Osteosarcoma. *Colloids Surf. B: Biointerfaces* 190, 110891. doi:10.1016/j.colsurfb.2020.110891

Iram, S., Zahera, M., Khan, S., Khan, I., Syed, A., Ansary, A. A., et al. (2017). Gold Nanoconjugates Reinforce the Potency of Conjugated Cisplatin and Doxorubicin. *Colloids Surf. B: Biointerfaces* 160, 254–264. doi:10.1016/j.colsurfb.2017.09.017

Jahan, K., and Tabrizian, M. (2016). Composite Biopolymers for Bone Regeneration Enhancement in Bony Defects. *Biomater. Sci.* 4, 25–39. doi:10.1039/c5bm00163c

Ju, P., Liang, R., Lee, Y., Zeng, Z., and Chuang, S. (2015). Differential Cytotoxic Effects of Gold Nanoparticles in Different Mammalian Cell Lines. *J. Hazard. Mater.* 264, 303–312. doi:10.1016/j.jhazmat.2013.11.031

Khan, S. N., Cammisa, F. P., Sandhu, H. S., Diwan, A. D., Girardi, F. P., and Lane, J. M. (2005). The Biology of Bone Grafting. *J. Am. Acad. Orthopaedic Surgeons* 13, 77–86. doi:10.5435/00124635-200501000-00010

Kim, G. J., and Nie, S. (2005). Targeted Cancer Nanotherapy. *Mater. Today* 8, 28–33. doi:10.1016/S1369-7021(05)71034-8

Kim, H., Yang, G. H., Choi, C. H., Cho, Y. S., and Kim, G. (2018). Gelatin/PVA Scaffolds Fabricated Using a 3D-Printing Process Employed with a Low-Temperature Plate for Hard Tissue Regeneration: Fabrication and Characterizations. *Int. J. Biol. Macromolecules* 120, 119–127. doi:10.1016/j.ijbiomac.2018.07.159

Kim, J.-Y., Ahn, G., Kim, C., Lee, J.-S., Lee, I.-G., An, S.-H., et al. (2018). Synergistic Effects of Beta Tri-calcium Phosphate and Porcine-Derived Decellularized Bone Extracellular Matrix in 3D-Printed Polycaprolactone Scaffold on Bone Regeneration. *Macromol. Biosci.* 18, 1800025. doi:10.1002/mabi.201800025

Komiya, S., Gebhardt, M. C., Mangham, D. C., and Inoue, A. (1998). Role of Glutathione in Cisplatin Resistance in Osteosarcorna Cell Lines. *J. Orthop. Res.* 16, 15–22. doi:10.1002/jor.1100160104

Kovács, D., Igaz, N., Keskeny, C., Bélteky, P., Tóth, T., Gáspár, R., et al. (2016). Silver Nanoparticles Defeat P53-Positive and P53-Negative Osteosarcoma Cells by Triggering Mitochondrial Stress and Apoptosis. *Sci. Rep.* 6, 1–13. doi:10.1038/srep27902

Kuttappan, S., Mathew, D., and Nair, M. B. (2016). Biomimetic Composite Scaffolds Containing Bioceramics and Collagen/gelatin for Bone Tissue Engineering - A Mini Review. *Int. J. Biol. Macromolecules* 93, 1390–1401. doi:10.1016/j.ijbiomac.2016.06.043

Lai, Y., Li, Y., Cao, H., Long, J., Wang, X., Li, L., et al. (2019). Osteogenic Magnesium Incorporated into PLGA/TCP Porous Scaffold by 3D Printing for Repairing Challenging Bone Defect. *Biomaterials* 197, 207–219. doi:10.1016/j.biomaterials.2019.01.013

Lavrador, P., Gaspar, V. M., and Mano, J. F. (2018). Stimuli-responsive Nanocarriers for Delivery of Bone Therapeutics - Barriers and Progresses. *J. Controlled Release* 273, 51–67. doi:10.1016/j.jconrel.2018.01.021

Lee, H., Yang, G. H., Kim, M., Lee, J., Huh, J., and Kim, G. (2018). Fabrication of Micro/nanoporous collagen/dECM/silk-Fibroin Biocomposite Scaffolds Using a Low Temperature 3D Printing Process for Bone Tissue Regeneration. *Mater. Sci. Eng. C* 84, 140–147. doi:10.1016/j.msec.2017.11.013

Lee, S., and Jun, B.-H. (2019). Silver Nanoparticles: Synthesis and Application for Nanomedicine. *Int. J. Mol. Sci.*, 20, 865. doi:10.3390/ijms20040865

Li, M., Du, C., Guo, N., Teng, Y., Meng, X., Sun, H., et al. (2019). Composition Design and Medical Application of Liposomes. *Eur. J. Med. Chem.* 164, 640–653. doi:10.1016/j.ejmech.2019.01.007

Li, Y., Bai, Y., Pan, J., Wang, H., Li, H., Xu, X., et al. (2019). A Hybrid 3D-Printed Aspirin-Laden Liposome Composite Scaffold for Bone Tissue Engineering. *J. Mater. Chem. B* 7, 619–629. doi:10.1039/C8TB02756K

Li, Y., Xiao, K., Zhu, W., Deng, W., and Lam, K. S. (2014). Stimuli-responsive Cross-Linked Micelles for On-Demand Drug Delivery against Cancers. *Adv. Drug Deliv. Rev.* 66, 58–73. doi:10.1016/j.addr.2013.09.008

Lin, K.-F., He, S., Song, Y., Wang, C.-M., Gao, Y., Li, J.-Q., et al. (2016). Low-Temperature Additive Manufacturing of Biomimic Three-Dimensional Hydroxyapatite/Collagen Scaffolds for Bone Regeneration. *ACS Appl. Mater. Inter.* 8, 6905–6916. doi:10.1021/acsami.6b00815

Liu, K., Li, W., Chen, S., Wen, W., Lu, L., Liu, M., et al. (2020). The Design, Fabrication and Evaluation of 3D Printed gHNTs/gMgO Whiskers/PLLA Composite Scaffold with Honeycomb Microstructure for Bone Tissue Engineering. *Composites B: Eng.* 192, 108001. doi:10.1016/j.compositesb.2020.108001

Liu, Y., Li, T., Ma, H., Zhai, D., Deng, C., Wang, J., et al. (2018). 3D-printed Scaffolds with Bioactive Elements-Induced Photothermal Effect for Bone Tumor Therapy. *Acta Biomater.* 73, 531–546. doi:10.1016/j.actbio.2018.04.014

Logithkumar, R., Keshavnarayan, A., Dhivya, S., Chawla, A., Saravanan, S., and Selvamurugan, N. (2016). A Review of Chitosan and its Derivatives in Bone Tissue Engineering. *Carbohydr. Polym.* 151, 172–188. doi:10.1016/j.carbpol.2016.05.049

Low, S. A., Yang, J., and Kopeček, J. (2014). Bone-targeted Acid-Sensitive Doxorubicin Conjugate Micelles as Potential Osteosarcoma Therapeutics. *Bioconjug. Chem.* 25, 2012–2020. doi:10.1021/bc500392x

Lu, Y., Gao, X., Cao, M., Wu, B., Su, L., Chen, P., et al. (2020). Interface Crosslinked mPEG-b-PAGE-b-PCL Triblock Copolymer Micelles with High Stability for Anticancer Drug Delivery. *Colloids Surf. B: Biointerfaces* 189, 110830. doi:10.1016/j.colsurfb.2020.110830

Lu, Y., Li, L., Lin, Z., Li, M., Hu, X., Zhang, Y., et al. (2018). Enhancing Osteosarcoma Killing and CT Imaging Using Ultrahigh Drug Loading and NIR-Responsive Bismuth Sulfide@Mesoporous Silica Nanoparticles. *Adv. Healthc. Mater.* 7, 1800602. doi:10.1002/adhm.201800602

Luetke, A., Meyers, P. A., Lewis, I., and Juergens, H. (2014). Osteosarcoma Treatment - where Do We Stand? A State of the Art Review. *Cancer Treat. Rev.* 40, 523–532. doi:10.1016/j.ctrv.2013.11.006

Luo, G., Ma, Y., Cui, X., Jiang, L., Wu, M., Hu, Y., et al. (2017). 13-93 Bioactive Glass/alginate Composite Scaffolds 3D Printed under Mild Conditions for Bone Regeneration. *RSC Adv.* 7, 11880–11889. doi:10.1039/c6ra27669e

Luo, Y., Li, Y., Qin, X., and Wa, Q. (2018). 3D Printing of Concentrated Alginate/gelatin Scaffolds with Homogeneous Nano Apatite Coating for Bone Tissue Engineering. *Mater. Des.* 146, 12–19. doi:10.1016/j.matdes.2018.03.002

Ma, D., Wang, Y., and Dai, W. (2018). Silk Fibroin-Based Biomaterials for Musculoskeletal Tissue Engineering. *Mater. Sci. Eng. C* 89, 456–469. doi:10.1016/j.msec.2018.04.062

Ma, H., Jiang, C., Zhai, D., Luo, Y., Chen, Y., Lv, F., et al. (2016). A Bifunctional Biomaterial with Photothermal Effect for Tumor Therapy and Bone Regeneration. *Adv. Funct. Mater.* 26, 1197–1208. doi:10.1002/adfm.201504142

Ma, H., Li, T., Huan, Z., Zhang, M., Yang, Z., Wang, J., et al. (2018). 3D Printing of High-Strength Bioscaffolds for the Synergistic Treatment of Bone Cancer. *NPG Asia Mater.* 10, 31–44. doi:10.1038/s41427-018-0015-8

Ma, Y., Hu, N., Liu, J., Zhai, X., Wu, M., Hu, C., et al. (2019). Three-Dimensional Printing of Biodegradable Piperazine-Based Polyurethane-Urea Scaffolds with Enhanced Osteogenesis for Bone Regeneration. *ACS Appl. Mater. Inter.* 11, 9415–9424. doi:10.1021/acsami.8b20323

Majeed, S., Aripin, F. H. B., Shoeb, N. S. B., Danish, M., Ibrahim, M. N. M., Hashim, R., et al. (2019). Bioengineered Silver Nanoparticles Capped with Bovine Serum Albumin and its Anticancer and Apoptotic Activity against Breast, Bone and Intestinal colon Cancer Cell Lines. *Mater. Sci. Eng. C* 102, 254–263. doi:10.1016/j.msec.2019.04.041

Martin, V., and Bettencourt, A. (2018). Bone Regeneration: Biomaterials as Local Delivery Systems with Improved Osteoinductive Properties. *Mater. Sci. Eng. C* 82, 363–371. doi:10.1016/j.msec.2017.04.038

Martin, V., Ribeiro, I. A., Alves, M. M., Gonçalves, L., Claudio, R. A., Grenho, L., et al. (2019). Engineering a Multifunctional 3D-Printed PLA-Collagen-Minocycline-nanoHydroxyapatite Scaffold with Combined Antimicrobial and Osteogenic Effects for Bone Regeneration. *Mater. Sci. Eng. C* 101, 15–26. doi:10.1016/j.msec.2019.03.056

Martínez-Carmona, M., Lozano, D., Colilla, M., and Vallet-Regí, M. (2018). Lectin-conjugated pH-Responsive Mesoporous Silica Nanoparticles for Targeted Bone Cancer Treatment. *Acta Biomater.* 65, 393–404. doi:10.1016/j.actbio.2017.11.007

Martínez-Vázquez, F. J., Cabañas, M. V., Paris, J. L., Lozano, D., and Vallet-Regí, M. (2015). Fabrication of Novel Si-Doped Hydroxyapatite/gelatine Scaffolds by Rapid Prototyping for Drug Delivery and Bone Regeneration. *Acta Biomater.* 15, 200–209. doi:10.1016/j.actbio.2014.12.021

Marzec, M., Kucińska-Lipka, J., Kalaszczyńska, I., and Janik, H. (2017). Development of Polyurethanes for Bone Repair. *Mater. Sci. Eng. C* 80, 736–747. doi:10.1016/j.msec.2017.07.047

Melim, C., Jarak, I., Veiga, F., and Figueiras, A. (2020). The Potential of Micelleplexes as a Therapeutic Strategy for Osteosarcoma Disease. *3 Biotech.* 10, 1–15. doi:10.1007/s13205-020-2142-5

Melke, J., Midha, S., Ghosh, S., Ito, K., and Hofmann, S. (2016). Silk Fibroin as Biomaterial for Bone Tissue Engineering. *Acta Biomater.* 31, 1–16. doi:10.1016/j.actbio.2015.09.005

Meshkini, A., and Oveisi, H. (2017). Methotrexate-F127 Conjugated Mesoporous Zinc Hydroxyapatite as an Efficient Drug Delivery System for Overcoming Chemotherapy Resistance in Osteosarcoma Cells. *Colloids Surf. B: Biointerfaces* 158, 319–330. doi:10.1016/j.colsurfb.2017.07.006

Mondal, S., Manivasagan, P., Bharathiraja, S., Santha Moorthy, M., Nguyen, V., Kim, H., et al. (2017). Hydroxyapatite Coated Iron Oxide Nanoparticles: A Promising Nanomaterial for Magnetic Hyperthermia Cancer Treatment. *Nanomaterials* 7, 426. doi:10.3390/nano7120426

Mondal, S., Nguyen, T. P., Pham, V. H., Hoang, G., Manivasagan, P., Kim, M. H., et al. (2020). Hydroxyapatite Nano Bioceramics Optimized 3D Printed Poly Lactic Acid Scaffold for Bone Tissue Engineering Application. *Ceramics Int.* 46, 3443–3455. doi:10.1016/j.ceramint.2019.10.057

Montalbano, G., Fiorilli, S., Caneschi, A., and Vitale-Brovarone, C. (2018). Type I Collagen and Strontium-Containing Mesoporous Glass Particles as Hybrid Material for 3D Printing of Bone-like Materials. *Materials* 11, 700. doi:10.3390/ma11050700

Murugan, B., and Krishnan, U. M. (2018). Chemoresponsive Smart Mesoporous Silica Systems - an Emerging Paradigm for Cancer Therapy. *Int. J. Pharmaceutics* 553, 310–326. doi:10.1016/j.ijpharm.2018.10.026

Narayanan, G., Vernekar, V. N., Kuyinu, E. L., and Laurencin, C. T. (2016). Poly (Lactic Acid)-Based Biomaterials for Orthopaedic Regenerative Engineering. *Adv. Drug Deliv. Rev.* 107, 247–276. doi:10.1016/j.addr.2016.04.015

Noy, J.-M., Lu, H., Hogg, P. J., Yang, J.-L., and Stenzel, M. (2018). Direct Polymerization of the Arsenic Drug PENAO to Obtain Nanoparticles with High Thiol-Reactivity and Anti-cancer Efficiency. *Bioconjug. Chem.* 29, 546–558. doi:10.1021/acs.bioconjchem.8b00032

Özel, F., Karaagac, O., Tokay, E., Köçkar, F., and Köçkar, H. (2019). A Simple Way to Synthesize Tartaric Acid, Ascorbic Acid and Their Mixture Coated Superparamagnetic Iron Oxide Nanoparticles with High Saturation Magnetisation and High Stability against Oxidation: Characterizations and Their Biocompatibility Studies. *J. Magnetism Magn. Mater.* 474, 654–660. doi:10.1016/j.jmmm.2018.11.025

Paris, J. L., Manzano, M., Cabañas, M. V., and Vallet-Regí, M. (2018). Mesoporous Silica Nanoparticles Engineered for Ultrasound-Induced Uptake by Cancer Cells. *Nanoscale* 10, 6402–6408. doi:10.1039/c8nr00693h

Park, J., Lee, S. J., Lee, H., Park, S. A., and Lee, J. Y. (2018). Three Dimensional Cell Printing with Sulfated Alginate for Improved Bone Morphogenetic Protein-2 Delivery and Osteogenesis in Bone Tissue Engineering. *Carbohydr. Polym.* 196, 217–224. doi:10.1016/j.carbpol.2018.05.048

Pei, P., Wei, D., Zhu, M., Du, X., and Zhu, Y. (2017). The Effect of Calcium Sulfate Incorporation on Physiochemical and Biological Properties of 3D-Printed Mesoporous Calcium Silicate Cement Scaffolds. *Microporous Mesoporous Mater.* 241, 11–20. doi:10.1016/j.micromeso.2016.11.031

Pérez-Rigueiro, J., Elices, M., Llorca, J., and Viney, C. (2001). Tensile Properties of Silkworm Silk Obtained by Forced Silking. *Appl. Polym. Sci.* 82, 1928–1935. doi:10.1002/app.2038

Pizzorno, J. (2014). Glutathione!. *Integr. Med. A Clin. J.* 13, 8–12.

Popescu, R. C., Andronescu, E., Vasile, B. S., Truşcă, R., Boldeiu, A., Mogoantă, L., et al. (2017). Fabrication and Cytotoxicity of Gemcitabine-Functionalized Magnetite Nanoparticles. *Molecules* 22, 1080. doi:10.3390/molecules22071080

Prasadh, S., and Wong, R. C. W. (2018). Unraveling the Mechanical Strength of Biomaterials Used as a Bone Scaffold in Oral and Maxillofacial Defects. *Oral Sci. Int.* 15, 48–55. doi:10.1016/S1348-8643(18)30005-3

Raghubir, M., Rahman, C., Fang, J., Matsui, H., and Mahajan, S. (2020). Osteosarcoma Growth Suppression by Riluzole Delivery via Iron Oxide Nanocage in Nude Mice. *Oncol. Rep.* 43, 169–176. doi:10.3892/or.2019.7420

Rahim, M., Iram, S., Khan, M. S., Khan, M. S., Shukla, A. R., Srivastava, A. K., et al. (2014). Glycation-assisted Synthesized Gold Nanoparticles Inhibit Growth of Bone Cancer Cells. *Colloids Surf. B: Biointerfaces* 117, 473–479. doi:10.1016/j.colsurfb.2013.12.008

Rainer, A., Giannitelli, S. M., Abbruzzese, F., Traversa, E., Licoccia, S., and Trombetta, M. (2008). Fabrication of Bioactive Glass-Ceramic Foams Mimicking Human Bone Portions for Regenerative Medicine. *Acta Biomater.* 4, 362–369. doi:10.1016/j.actbio.2007.08.007

Raj, S., Khurana, S., Choudhari, R., Kesari, K. K., Kamal, M. A., Garg, N., et al. (2021). Specific Targeting Cancer Cells with Nanoparticles and Drug Delivery in Cancer Therapy. *Semin. Cancer Biol.* 69, 166–177. doi:10.1016/j.semcancer.2019.11.002

Rajabnia, T., and Meshkini, A. (2018). Fabrication of Adenosine 5′-Triphosphate-Capped Silver Nanoparticles: Enhanced Cytotoxicity Efficacy and Targeting Effect against Tumor Cells. *Process Biochem.* 65, 186–196. doi:10.1016/j.procbio.2017.11.003

Rajzer, I., Kurowska, A., Jabłoński, A., Jatteau, S., Śliwka, M., Ziąbka, M., et al. (2018). Layered Gelatin/PLLA Scaffolds Fabricated by Electrospinning and 3D Printing- for Nasal Cartilages and Subchondral Bone Reconstruction. *Mater. Des.* 155, 297–306. doi:10.1016/j.matdes.2018.06.012

Rastinehad, A. R., Anastos, H., Wajswol, E., Winoker, J. S., Sfakianos, J. P., Doppalapudi, S. K., et al. (2019). Gold Nanoshell-Localized Photothermal Ablation of Prostate Tumors in a Clinical Pilot Device Study. *Proc. Natl. Acad. Sci. USA* 116, 18590–18596. doi:10.1073/pnas.1906929116

Rayamajhi, S., Marchitto, J., Nguyen, T. D. T., Marasini, R., Celia, C., Aryal, S., et al. (2020). pH-responsive Cationic Liposome for Endosomal Escape Mediated Drug Delivery. *Colloids Surf. B: Biointerfaces* 188, 110804. doi:10.1016/j.colsurfb.2020.110804

Reith, J. D. (2018). "Bone and Joints," in *Rosai And Ackerman's Surgical Pathology*. Elsevier, 1740–1809. Available at: https://www.clinicalkey.com/#!/content/book/3-s2.0-B9780323263399000408?scrollTo=%23top.

Ribas, R. G., Schatkoski, V. M., Montanheiro, T. L. d. A., de Menezes, B. R. C., Stegemann, C., Leite, D. M. G., et al. (2019). Current Advances in Bone Tissue Engineering Concerning Ceramic and Bioglass Scaffolds: A Review. *Ceramics Int.* 45, 21051–21061. doi:10.1016/j.ceramint.2019.07.096

Roberts, T. T., and Rosenbaum, A. J. (2012). Bone Grafts, Bone Substitutes and Orthobiologics. *Organogenesis* 8, 114–124. doi:10.4161/org.23306

Roosa, S. M. M., Kemppainen, J. M., Moffitt, E. N., Krebsbach, P. H., and Hollister, S. J. (2010). The Pore Size of Polycaprolactone Scaffolds Has Limited Influence on Bone Regeneration in Anin Vivomodel. *J. Biomed. Mater. Res.* 92A, 359–368. doi:10.1002/jbm.a.32381

Ruttala, H. B., Ramasamy, T., Madeshwaran, T., Hiep, T. T., Kandasamy, U., Oh, K. T., et al. (2018). Emerging Potential of Stimulus-Responsive Nanosized Anticancer Drug Delivery Systems for Systemic Applications. *Arch. Pharm. Res.* 41, 111–129. doi:10.1007/s12272-017-0995-x

Sábio, R. M., Meneguin, A. B., Ribeiro, T. C., Silva, R. R., and Chorilli, M. (2019). New Insights towards Mesoporous Silica Nanoparticles as a Technological Platform for Chemotherapeutic Drugs Delivery. *Int. J. Pharmaceutics* 564, 379–409. doi:10.1016/j.ijpharm.2019.04.067

Sachlos, E., Phil, D., Gotora, D., Czernuszka, J. a. N. T., and Ph, D. (2006). Collagen Scaffolds Reinforced with Biomimetic Composite Nano-Sized Carbonate-Substituted Hydroxyapatite Crystals and Shaped by Rapid Prototyping to Contain Internal Microchannels. *Tissue Eng.* 12, 2479. doi:10.1089/ten.2006.12.2479

Samavedi, S., Whittington, A. R., and Goldstein, A. S. (2013). Calcium Phosphate Ceramics in Bone Tissue Engineering: A Review of Properties and Their Influence on Cell Behavior. *Acta Biomater.* 9, 8037–8045. doi:10.1016/j.actbio.2013.06.014

Sánchez-Paradinas, S., Pérez-Andrés, M., Almendral-Parra, M. J., Rodríguez-Fernández, E., Millán, Á., Palacio, F., et al. (2014). Enhanced Cytotoxic Activity of Bile Acid Cisplatin Derivatives by Conjugation with Gold Nanoparticles. *J. Inorg. Biochem.* 131, 8–11. doi:10.1016/j.jinorgbio.2013.10.021

Santoro, M., Tatara, A. M., and Mikos, A. G. (2014). Gelatin Carriers for Drug and Cell Delivery in Tissue Engineering. *J. Control. Release* 190, 210–218. doi:10.1016/j.jconrel.2014.04.014

Saravanan, S., Leena, R. S., and Selvamurugan, N. (2016). Chitosan Based Biocomposite Scaffolds for Bone Tissue Engineering. *Int. J. Biol. Macromol.* 93, 1354–1365. doi:10.1016/j.ijbiomac.2016.01.112

Sarkar, N., and Bose, S. (2019). Liposome-Encapsulated Curcumin-Loaded 3D Printed Scaffold for Bone Tissue Engineering. *ACS Appl. Mater. Inter.* 11, 17184–17192. doi:10.1021/acsami.9b01218

Shuai, C., Cheng, Y., Yang, W., Feng, P., Yang, Y., He, C., et al. (2020). Magnetically Actuated Bone Scaffold: Microstructure, Cell Response and Osteogenesis. *Composites Part B: Eng.* 192, 107986. doi:10.1016/j.compositesb.2020.107986

Singh, P., Pandit, S., Mokkapati, V. R. S. S., Garg, A., Ravikumar, V., and Mijakovic, I. (2018). Gold Nanoparticles in Diagnostics and Therapeutics for Human Cancer. *Int. J. Mol. Sci.* 19, 1979. doi:10.3390/ijms19071979

Song, Y., Lin, K., He, S., Wang, C., Zhang, S., Li, D., et al. (2018). Nano-biphasic Calcium Phosphate/polyvinyl Alcohol Composites with Enhanced Bioactivity for Bone Repair via Low-Temperature Three-Dimensional Printing and Loading with Platelet-Rich Fibrin. *Int. J. Nanomedicine.* Vol.13, 505–523. doi:10.2147/IJN.S152105

Steckiewicz, K. P., Barcińska, E., Sobczak, K., Tomczyk, E., Wójcik, M., and Inkielewicz-Stepniak, I. (2020). Assessment of Anti-tumor Potential and Safety of Application of Glutathione Stabilized Gold Nanoparticles Conjugated with Chemotherapeutic. *Int. J. Med. Sci.* 17, 824, doi:10.7150/ijms.40827

Steckiewicz, K. P., Barcinska, E., Malankowska, A., Zauszkiewicz–Pawlak, A., Nowaczyk, G., Zaleska-Medynska, A., et al. (2019). Impact of Gold Nanoparticles Shape on Their Cytotoxicity against Human Osteoblast and Osteosarcoma in *In Vitro* Model. Evaluation of the Safety of Use and Anti-cancer Potential. *J. Mater. Sci. Mater. Med.* 30, 1–15. doi:10.1007/s10856-019-6221-2

Su, K., and Wang, C. (2015). Recent Advances in the Use of Gelatin in Biomedical Research. *Biotechnol. Lett.* 37, 2139–2145. doi:10.1007/s10529-015-1907-0

Tajbakhsh, S., and Hajiali, F. (2017). A Comprehensive Study on the Fabrication and Properties of Biocomposites of Poly(lactic Acid)/ceramics for Bone Tissue Engineering. *Mater. Sci. Eng. C* 70, 897–912. doi:10.1016/j.msec.2016.09.008

Tapeinos, C., Battaglini, M., Prato, M., La Rosa, G., Scarpellini, A., and Ciofani, G. (2018). CeO2 Nanoparticles-Loaded pH-Responsive Microparticles with Antitumoral Properties as Therapeutic Modulators for Osteosarcoma. *ACS Omega* 3, 8952–8962. doi:10.1021/acsomega.8b01060

Tarafder, S., Balla, V. K., Davies, N. M., Bandyopadhyay, A., and Bose, S. (2013). Microwave-sintered 3D Printed Tricalcium Phosphate Scaffolds for Bone Tissue Engineering. *J. Tissue Eng. Regen. Med.* 7, 631–641. doi:10.1002/term.555

The American Cancer Society (2020). Key Statistics for Osteosarcoma. Available at: https://www.cancer.org/cancer/osteosarcoma/about/key-statistics.html (Accessed February 10, 2020).

Torres, M. L., Fernandez, J. M., Dellatorre, F. G., Cortizo, A. M., and Oberti, T. G. (2019). Purification of Alginate Improves its Biocompatibility and Eliminates Cytotoxicity in Matrix for Bone Tissue Engineering. *Algal Res.* 40, 101499. doi:10.1016/j.algal.2019.101499

Toy, P. C., and Heck, R. K. (2017). General Principles of Tumors. in *Campbell's Operative Orthopaedics*. (Philadelphia: Elsevier), 829–895. Available at: https://0-www-clinicalkey-com.innopac.wits.ac.za/#!/content/book/3-s2.0-B9780323374620000240?scrollTo=%23top.

Tudose, M., Culita, D. C., Musuc, A. M., Somacescu, S., Ghica, C., Chifiriuc, M. C., et al. (2017). Lipoic Acid Functionalized SiO2@Ag Nanoparticles. Synthesis, Characterization and Evaluation of Biological Activity. *Mater. Sci. Eng. C* 79, 499–506. doi:10.1016/j.msec.2017.05.083

Usta, M., Piech, D. L., MacCrone, R. K., and Hillig, W. B. (2003). Behavior and Properties of Neat and Filled Gelatins. *Biomaterials* 24, 165–172. doi:10.1016/S0142-9612(02)00274-0

Vegerhof, A., Barnoy, E., Motiei, M., Malka, D., Danan, Y., Zalevsky, Z., et al. (2016). Targeted Magnetic Nanoparticles for Mechanical Lysis of Tumor Cells by Low-Amplitude Alternating Magnetic Field. *Materials* 9, 943. doi:10.3390/ma9110943

Velioglu, Z. B., Pulat, D., Demirbakan, B., Ozcan, B., Bayrak, E., and Erisken, C. (2019). 3D-printed Poly(lactic Acid) Scaffolds for Trabecular Bone Repair and Regeneration: Scaffold and Native Bone Characterization. *Connect. Tissue Res.* 60, 274–282. doi:10.1080/03008207.2018.1499732

Venkatesan, J., Bhatnagar, I., Manivasagan, P., Kang, K.-H., and Kim, S.-K. (2015). Alginate Composites for Bone Tissue Engineering: A Review. *Int. J. Biol. Macromol.* 72, 269–281. doi:10.1016/j.ijbiomac.2014.07.008

Venkatraman, S. K., and Swamiappan, S. (2020). Review on Calcium- and Magnesium-Based Silicates for Bone Tissue Engineering Applications. *J. Biomed. Mater. Res.* 108, 1546–1562. doi:10.1002/jbm.a.36925

Wang, C., Huang, W., Zhou, Y., He, L., He, Z., Chen, Z., et al. (2020). 3D Printing of Bone Tissue Engineering Scaffolds. *Bioactive Mater.* 5, 82–91. doi:10.1016/j.bioactmat.2020.01.004

Wang, H., Zeng, X., Pang, L., Wang, H., Lin, B., Deng, Z., et al. (2020). Integrative Treatment of Anti-tumor/bone Repair by Combination of MoS2 Nanosheets with 3D Printed Bioactive Borosilicate Glass Scaffolds. *Chem. Eng. J.* 396, 125081. doi:10.1016/j.cej.2020.125081

Wang, S.-Y., Hu, H.-Z., Qing, X.-C., Zhang, Z.-C., and Shao, Z.-W. (2020). Recent Advances of Drug Delivery Nanocarriers in Osteosarcoma Treatment. *J. Cancer* 11, 69–82. doi:10.7150/jca.36588

Wang, Y.-J., Jeng, U.-S., and Hsu, S.-h. (2018). Biodegradable Water-Based Polyurethane Shape Memory Elastomers for Bone Tissue Engineering. *ACS Biomater. Sci. Eng.* 4, 1397–1406. doi:10.1021/acsbiomaterials.8b00091

Wei, J., Chen, F., Shin, J.-W., Hong, H., Dai, C., Su, J., et al. (2009). Preparation and Characterization of Bioactive Mesoporous Wollastonite - Polycaprolactone Composite Scaffold. *Biomaterials* 30, 1080–1088. doi:10.1016/j.biomaterials.2008.10.046

White, T. D., Black, M. T., and Folkens, P. A. (2012). Bone Biology and Variation. *Hum. Osteol.* 25, 42. doi:10.1016/b978-0-12-374134-9.50003-9

Wu, C., Luo, Y., Cuniberti, G., Xiao, Y., and Gelinsky, M. (2011). Three-dimensional Printing of Hierarchical and Tough Mesoporous Bioactive Glass Scaffolds with a Controllable Pore Architecture, Excellent Mechanical Strength and Mineralization Ability. *Acta Biomater.* 7, 2644–2650. doi:10.1016/j.actbio.2011.03.009

Xi, Y., Jiang, T., Yu, Y., Yu, J., Xue, M., Xu, N., et al. (2019). Dual Targeting Curcumin Loaded Alendronate-Hyaluronan- Octadecanoic Acid Micelles for Improving Osteosarcoma Therapy. *Int. J. Nanomedicine.* 14, 6425–6437. doi:10.2147/IJN.S211981

Xiao, D., Zhang, J., Zhang, C., Barbieri, D., Yuan, H., Moroni, L., et al. (2020). The Role of Calcium Phosphate Surface Structure in Osteogenesis and the Mechanisms Involved. *Acta Biomater.* 106, 22–33. doi:10.1016/j.actbio.2019.12.034

Xiong, L., Bi, J., Tang, Y., and Qiao, S. Z. (2016). Magnetic Core-Shell Silica Nanoparticles with Large Radial Mesopores for siRNA Delivery. *Small* 12, 4735–4742. doi:10.1002/smll.201600531

Yan, X., Yu, C., Zhou, X., Tang, J., and Zhao, D. (2004). Highly Ordered Mesoporous Bioactive Glasses with superior *In Vitro* Bone-Forming Bioactivities. *Angew. Chem. Int. Ed.* 43, 5980–5984. doi:10.1002/anie.200460598

Yan, Y., Chen, H., Zhang, H., Guo, C., Yang, K., Chen, K., et al. (2019). Vascularized 3D Printed Scaffolds for Promoting Bone Regeneration. *Biomaterials* 190-191, 97–110. doi:10.1016/j.biomaterials.2018.10.033

Yang, F., Wen, X., Ke, Q.-F., Xie, X.-T., and Guo, Y.-P. (2018). pH-responsive Mesoporous ZSM-5 Zeolites/chitosan Core-Shell Nanodisks Loaded with Doxorubicin against Osteosarcoma. *Mater. Sci. Eng. C* 85, 142–153. doi:10.1016/j.msec.2017.12.024

Yang, Z., Guo, Q., Cai, Y., Zhu, X., Zhu, C., Li, Y., et al. (2020). Poly(ethylene Glycol)-Sheddable Reduction-Sensitive Polyurethane Micelles for Triggered Intracellular Drug Delivery for Osteosarcoma Treatment. *J. Orthopaedic Transl.* 21, 57–65. doi:10.1016/j.jot.2019.11.001

Yang, Z., Hemar, Y., Hilliou, L., Gilbert, E. P., McGillivray, D. J., Williams, M. A. K., et al. (2016). Nonlinear Behavior of Gelatin Networks Reveals a Hierarchical Structure. *Biomacromolecules* 17, 590–600. doi:10.1021/acs.biomac.5b01538

Yin, X., Chi, Y., Guo, C., Feng, S., Liu, J., Sun, K., et al. (2017). Chitooligosaccharides Modified Reduction-Sensitive Liposomes: Enhanced Cytoplasmic Drug Delivery and Osteosarcomas-Tumor Inhibition in Animal Models. *Pharm. Res.* 34, 2172–2184. doi:10.1007/s11095-017-2225-0

Yin, X., Feng, S., Chi, Y., Liu, J., Sun, K., Guo, C., et al. (2018). Estrogen-functionalized Liposomes Grafted with Glutathione-Responsive Sheddable Chotooligosaccharides for the Therapy of Osteosarcoma. *Drug Deliv.* 25, 900–908. doi:10.1080/10717544.2018.1458920

Yu, Z., Chen, F., Qi, X., Dong, Y., Zhang, Y., Ge, Z., et al. (2018). Epidermal Growth Factor Receptor Aptamerconjugated Polymerlipid Hybrid Nanoparticles Enhance Salinomycin Delivery to Osteosarcoma and Cancer Stem Cells. *Exp. Ther. Med.* 15, 1247–1256. doi:10.3892/etm.2017.5578

Zaharin, H., Abdul Rani, A., Azam, F., Ginta, T., Sallih, N., Ahmad, A., et al. (2018). Effect of Unit Cell Type and Pore Size on Porosity and Mechanical Behavior of Additively Manufactured Ti6Al4V Scaffolds. *Materials* 11, 2402. doi:10.3390/ma11122402

Zelzer, E., McLean, W., Ng, Y.-S., Fukai, N., Reginato, A. M., Lovejoy, S., et al. (2002). Skeletal Defects in VEGF120/120 Mice Reveal Multiple Roles for VEGF in Skeletogenesis. *Development* 129, 1893–1904. doi:10.1242/dev.129.8.1893

Zhang, D., Wu, X., Chen, J., and Lin, K. (2018). The Development of Collagen Based Composite Scaffolds for Bone Regeneration. *Bioact. Mater.* 3, 129–138. doi:10.1016/j.bioactmat.2017.08.004

Zhang, J., Liu, W., Schnitzler, V., Tancret, F., and Bouler, J.-M. (2014). Calcium Phosphate Cements for Bone Substitution: Chemistry, Handling and Mechanical Properties. *Acta Biomater.* 10, 1035–1049. doi:10.1016/j.actbio.2013.11.001

Zhang, W., Shi, W., Wu, S., Kuss, M., Jiang, X., Untrauer, J. B., et al. (2020). 3D Printed Composite Scaffolds with Dual Small Molecule Delivery for Mandibular Bone Regeneration0–14jjm. *Biofabrication*, 12., 035020. doi:10.1088/1758-5090/ab906e

Zhang, Y., Zhai, D., Xu, M., Yao, Q., Chang, J., and Wu, C. (2016). 3D-printed Bioceramic Scaffolds with a Fe3O4/graphene Oxide Nanocomposite Interface for Hyperthermia Therapy of Bone Tumor Cells. *J. Mater. Chem. B* 4, 2874–2886. doi:10.1039/c6tb00390g

Zhang, Y., Zhai, D., Xu, M., Yao, Q., Zhu, H., Chang, J., et al. (2017). 3D-printed Bioceramic Scaffolds with Antibacterial and Osteogenic Activity. *Biofabrication* 9, 025037. doi:10.1088/1758-5090/aa6ed6

Zhao, H., Li, L., Ding, S., Liu, C., and Ai, J. (2018). Effect of Porous Structure and Pore Size on Mechanical Strength of 3D-Printed Comby Scaffolds. *Mater. Lett.* 223, 21–24. doi:10.1016/j.matlet.2018.03.205

Zhao, L., Bi, D., Qi, X., Guo, Y., Yue, F., Wang, X., et al. (2019). Polydopamine-based Surface Modification of Paclitaxel Nanoparticles for Osteosarcoma Targeted Therapy. *Nanotechnology* 30, 255101. doi:10.1088/1361-6528/ab055f

Zhu, M., Zhang, J., Zhao, S., and Zhu, Y. (2016). Three-dimensional Printing of Cerium-Incorporated Mesoporous Calcium-Silicate Scaffolds for Bone Repair. *J. Mater. Sci.* 51, 836–844. doi:10.1007/s10853-015-9406-1

Conflict of Interest: The authors declare that the research was conducted in the absence of any commercial or financial relationships that could be construed as a potential conflict of interest.